



Government of **Western Australia**  
Department of **Mines and Petroleum**

RECORD 2015/16

# 2<sup>ND</sup> LITHOSPHERE WORKSHOP 19–20 NOVEMBER 2015 THE UNIVERSITY OF WESTERN AUSTRALIA

compiled by  
W Gorczyk, K Gessner, Y Lu, and N Thébaud



Geological Survey  
of Western Australia



EXPLORATION  
INCENTIVE SCHEME



Centre for EXPLORATION  
TARGETING





Government of **Western Australia**  
Department of **Mines and Petroleum**

**Record 2015/16**

**2ND LITHOSPHERE WORKSHOP  
19–20 NOVEMBER 2015  
THE UNIVERSITY OF WESTERN AUSTRALIA**

**compiled by  
W Gorczyk, K Gessner, Y Lu, and N Thébaud**

**Perth 2015**



**Geological Survey of  
Western Australia**

**MINISTER FOR MINES AND PETROLEUM**  
**Hon. Bill Marmion MLA**

**DIRECTOR GENERAL, DEPARTMENT OF MINES AND PETROLEUM**  
**Richard Sellers**

**EXECUTIVE DIRECTOR, GEOLOGICAL SURVEY OF WESTERN AUSTRALIA**  
**Rick Rogerson**

#### **REFERENCE**

**The recommended reference for this publication is:**

Gorczyk, W, Gessner, K, Lu, Y and Thébaud, N (compilers) 2015, 2nd lithosphere workshop, 19–20 November 2015, The University of Western Australia: Geological Survey of Western Australia, Record 2015/16, 37p.

**National Library of Australia Card Number and ISBN 978-1-74168-658-6**

#### **About this publication**

This Record presents the final abstracts for the 2<sup>nd</sup> lithosphere workshop which was held 19–20 November 2015 at The University of Western Australia. The scientific content of the Record is the responsibility of the authors. No editing has been undertaken by GSWA.



#### **Published 2015 by Geological Survey of Western Australia**

This Record is published in digital format (PDF) and is available online at <[www.dmp.wa.gov.au/GSWApublications](http://www.dmp.wa.gov.au/GSWApublications)>.

#### **Disclaimer**

This product was produced using information from various sources. The Department of Mines and Petroleum (DMP) and the State cannot guarantee the accuracy, currency or completeness of the information. DMP and the State accept no responsibility and disclaim all liability for any loss, damage or costs incurred as a result of any use of or reliance whether wholly or in part upon the information provided in this publication or incorporated into it by reference.

#### **Further details of geological products and maps produced by the Geological Survey of Western Australia are available from:**

Information Centre  
Department of Mines and Petroleum  
100 Plain Street  
EAST PERTH WESTERN AUSTRALIA 6004  
Telephone: +61 8 9222 3459 Facsimile: +61 8 9222 3444  
[www.dmp.wa.gov.au/GSWApublications](http://www.dmp.wa.gov.au/GSWApublications)

## Contents

Continental crust on Mars: pieces of evidence and implication.....	1
<i>David Baratoux</i>	
Crust–mantle interactions in hot orogens characterised by counterclockwise P–T–t paths and slow cooling .....	3
<i>Mike Brown</i>	
Transport of metals in hydrothermal fluids .....	5
<i>Joel Brugger</i>	
Australian Architecture Reference Model (AusARM): Towards constraining the spatial and temporal evolution of the lithosphere .....	7
<i>Karol Czarnota</i>	
Geophysical Detection of Mineral Systems in the Deep Crust and Upper Mantle.....	9
<i>Mike Dentith</i>	
Sulfur and metal fertilization of the lower continental crust.....	10
<i>Marco Fiorentini</i>	
Evolution of the lithospheric mantle by melt/rock interaction and its effects on the composition of lithosphere-derived volcanic melts.....	11
<i>Stephen Foley</i>	
Constraints on kimberlite ascent mechanisms revealed by phlogopite compositions in kimberlites and mantle xenoliths .....	13
<i>Andrea Giuliani</i>	
Neutral-Buoyancy Rule Over-Ruled: Crustal Underplating by Buoyant Magmas during Orogeny .....	14
<i>Robert Loucks</i>	
Magmatic gas reactions in sub-volcanic arcs.....	16
<i>John Mavrogenes</i>	
The smoothness and shapes of chondrite-normalized Rare Earth Element patterns in basalts.....	18
<i>Hugh O'Neill</i>	
Magnetotelluric imaging of the Earth across scales.....	19
<i>Stephen Thiel</i>	
Secular change in Archean crust formation recorded in Western Australia .....	21
<i>Huaiyu Yuan</i>	

## Poster abstracts

Trace element analysis on sulphides in olivine-phyric Shergottites: constraints on the behaviour of siderophile-chalcophile elements and sulphur in Martian magmatic systems .....	24
<i>Raphael J. Baumgartner</i>	
Ruthenium in spinel from Chassignite and olivine-phyric Shergottite meteorites: constraints on the behavior of platinum-group elements and sulphur in Martian magmatic systems .....	25
<i>Raphael J. Baumgartner</i>	
Cassiterite as a multiprocess recorder in Sn bearing systems .....	26
<i>Jason Bennett</i>	
Unravelling crustal growth and geodynamics in the Meso to Neoarchaeon using U-Pb-O isotopes in zircons and stratigraphic reconstructions from the Marmion Terrane (3.0 Ga) .....	27
<i>Katharina Björkman</i>	
The Arabian-Nubian Shield (8.50-5.50 Ga) as an analogue for the Birimian Orogen (2.35-2.05 Ga)? .....	28
<i>Mikael Grenholm</i>	
In-situ U-Pb, O and Hf isotopic compositions of detrital zircons from the North Australian Craton .....	29
<i>Linda Iaccheri</i>	
Geochronology and lithostratigraphy of the Siguiri district: implications for gold mineralisation in the Siguiri Basin (Guinea, West Africa) .....	30
<i>Erwann Lebrun</i>	
The tectono-magmatic evolution of the Kédougou-Kénieba inlier, West Africa: new insights from the Sadiola-Yatela gold district .....	32
<i>Quentin Masurel</i>	
Melt generation during failed rift development – Insights from numerical modeling .....	33
<i>Mark A Munro</i>	
Crustal Architecture and Under Cover Exploration: The Granites – Tanami Orogen Example .....	34
<i>David B Stevenson</i>	
Kimberlitic Plumbing System: One-Time Incident or Long-Term Relation? .....	35
<i>Irina Tretiakova</i>	
Can auriferous fluids produce their own pathways via porosity forming reactions? An insight from the Mick Adam gold deposit, Yilgarn Craton, Western Australia .....	37
<i>James Warren</i>	

## PROGRAM: 2<sup>nd</sup> Lithosphere workshop, 19–20 November, 2015, UWA, Perth

### Day1

#### Imaging the architecture and composition of the deep lithosphere - how are we advancing

8.00 – 9.00	Registration	
9.00 – 9.15	<b>Campbell McCuaig</b>	Opening remarks
9.15 – 10.00	<b>Stephen Thiel</b>	Magnetotelluric imaging of the earth across scales
10.00 – 10.45	<b>Mike Dentith</b>	Geophysical Detection of Mineral Systems in the Deep Crust and Upper Mantle
10.45 – 11.15	Morning tea	
11.15 – 12.00	<b>David Baratoux</b>	Pieces of evidence for continental crust on Mars and implications for the structure of the Martian crust
12.00 – 13.00	Lunch	
13.00 – 13.45	<b>Karol Czarnota</b>	Australian Architecture Reference Model (AusARM): Towards constraining the spatial and temporal evolution of the lithosphere
13.45 – 14.30	<b>Huaiyu Yuan</b>	Secular change in Archean crust formation recorded in Western Australia
14.30 – 15.15	<b>Andrea Giuliani</b>	Constraints on kimberlite ascent mechanisms revealed by phlogopite compositions in kimberlites and mantle xenoliths
15.15 – 15.45	Afternoon tea	
15.45 – 17.00	POSTERS	5 min posters presentations in the lecture room followed by poster session

### DAY 2

#### Metal-fluid-magma-mineral interaction partitioning in the lithosphere - what do we know and not know?

8.30 – 9.15	<b>Mike Brown</b>	Crust–mantle interactions in hot orogens characterised by counterclockwise P–T–t paths and slow cooling
9.15 – 10.00	<b>Robert Loucks</b>	Neutral-Buoyancy Rule Over-Ruled: Crustal Underplating by Buoyant Magmas during Orogeny
10.00 – 10.30	Morning tea	
10.30 – 11.15	<b>Marco Fiorentini</b>	Sulfur and metal fertilization of the lower continental crust
11.15 – 12.00	<b>Joel Brugger</b>	Transport of metals in hydrothermal fluids
12.00 – 13.30	Lunch + POSTERS	
13.30 – 14.15	<b>Hugh O'Neill</b>	The smoothness and shapes of chondrite-normalized Rare Earth Element patterns in basalts
14.15 – 15.00	<b>John Mavrogenes</b>	Magmatic gas reactions in sub-volcanic arcs
15.00 – 15.30	Afternoon tea	
15.30 – 16.15	<b>Stephen Foley</b>	Evolution of the lithospheric mantle by melt/rock interaction and its effects on the composition of lithosphere-derived volcanic melts
16.15 – 16.30	<b>Campbell McCuaig</b>	Closing remarks

### Poster session

	<b>Name</b>	<b>Title</b>
1	<b>Raphael J. Baumgartne</b>	Trace element analysis on sulphides in olivine-phyric Shergottites: constraints on the behaviour of siderophile-chalcophile elements and sulphur in Martian magmatic systems
2	<b>Raphael J. Baumgartne</b>	Ruthenium in spinel from Chassignite and olivine-phyric Shergottite meteorites: constraints on the behavior of platinum-group elements and sulphur in Martian magmatic systems
3	<b>Jason Bennett</b>	Cassiterite as a multiprocess recorder in Sn bearing systems
4	<b>Katharina Björkman</b>	Unravelling crustal growth and geodynamics in the Meso to Neoproterozoic using U-Pb-O isotopes in zircons and stratigraphic reconstructions from the Marmion Terrane (3.0 Ga)
5	<b>Mikael Grenholm</b>	The Arabian-Nubian Shield (8.50–5.50 Ga) as an analogue for the Birimian Orogen (2.35–2.05 Ga)?
6	<b>Linda Iaccheri</b>	In-situ U-Pb, O and Hf isotopic compositions of detrital zircons from the North Australian Craton
7	<b>Erwann Lebrun</b>	Geochronology and lithostratigraphy of the Siguiri district: implications for gold mineralisation in the Siguiri Basin (Guinea, West Africa)
8	<b>Quentin Masurel</b>	The tectono-magmatic evolution of the Kédougou-Kénieba inlier, West Africa: new insights from the Sadiola-Yatela gold district.
9	<b>Mark A. Munro</b>	Melt generation during failed rift development – Insights from numerical modeling
10	<b>David B Stevenson</b>	Crustal Architecture and Under Cover Exploration: The Granites – Tanami Orogen Example
11	<b>Irina Tretiakova</b>	Kimberlitic Plumbing System: One-Time Incident or Long-Term Relation?
12	<b>James Warren</b>	Can auriferous fluids produce their own pathways via porosity forming reactions? An insight from the Mick Adam gold deposit, Yilgarn Craton, Western Australia.



## Continental crust on Mars: pieces of evidence and implication

by

D. Baratoux\*

The formation of the continental crust is certainly one of the most interesting things that ever happened to the Earth. Without continental crust, Earth would have been a drab waterworld enveloped by a stagnant basaltic crust and covered by a global ocean (Arndt et al. 2014). This description of the Earth without continental crust would actually apply to the representations of the Martian crust and to the ancient surface environment that had emerged in the beginning of this century after several decades of exploration with rovers and orbiters providing in-situ chemical analyses and high-resolution satellite imagery and spectroscopy. In detail, the surface of Mars – with an implicit extrapolation to the entire crust – was until recently considered to be a basalt-dominated world. It was shown that the composition of the basaltic provinces reflects the slow cooling of the planet and thickening of lithosphere in the framework of a homogeneously convecting mantle below a stagnant lid (Baratoux et al. 2011, Baratoux et al. 2013, Grott et al. 2013, Filiberto and Dasgupta 2015).

However, a series of recent studies have seriously challenged this vision, at least for the earliest history of the planet. These studies suggested that at least one continental crust forming event has also occurred on our neighboring planet and that some crustal rocks exposed at its surface of Mars are “petrologically reminiscent of Archaean trondhjemites, tonalites and granodiorites” (Sautter et al. 2015). I will first offer a review of the multiple pieces of evidence that a significant fraction of the crust of Mars is felsic, though most of this component may be buried under dense basaltic material. Direct evidence for differentiated rocks includes spectroscopic observations from the orbit (Wray et al. 2012, Carter and Poulet 2013), analyses of impact clasts from the Martian meteorite NWA7533 with 4.428 Ga old zircons (Humayun et al. 2013), and in-situ chemical and petrologic observations by the Rover Curiosity at Gale crater (Sautter et al. 2014, Sautter et al. 2015). However, it should be noted that these observations are restricted in space (essentially the highlands of the south hemisphere), and time (Noachian or Noachian/Hesperian boundary,

ie 4.5 – 3.7 Ga). Local occurrences of felsic rocks alone do not provide definitive evidence that these exceptional findings are significant for the lithospheric-scale evolution, and that Mars has experienced a general episode of continental crustal growth.

However, a few months before these findings, I noted that the commonly admitted crustal density and crustal thickness were not compatible with the assumption that the crust of Mars is basaltic in composition (Baratoux et al. 2014). Petrological constraints on the density of Martian basalts together with gravity data suggest the existence of a light crustal component that is essentially buried. I therefore postulate that the few occurrences of felsic or granitic material correspond to rare exposures of this light/felsic component that locally outcrops at the favor of tectonic contacts or impact craters. Moreover, I have re-examined recently global maps of K and Th concentrations in light of lessons learned recently from the analysis of radiometric data over the Northern Pilbara and West African cratons. This investigation reveals that the distribution of K and Th concentrations at the surface of Mars are compatible with disseminated occurrences of differentiated material (Baratoux et al., submitted) and offers another piece of evidence that local observations may be likely extrapolated at the crustal scale.

Future research will now focus on the search of additional exposure of this continental crust and detailed characterization of the petrology, chemistry and mineralogy of these enigmatic rocks. On Mars, like on Earth, partial melting of the mantle produces basalts. The formation of significant volume of granites on Earth results from hydrous re-melting of this basalt. The water can be present as a separate fluid phase or within hydrous minerals, but without it, abundant granitic magma does not form (Arndt et al. 2014). The mechanism and the geodynamic context(s) responsible for the formation of granitic magmas on Mars are unknown at present, but should be the topic of fascinating discussions, that should foster collaboration between specialists of the Archean and planetary scientists. Understanding the formation and structure of the crust of another planet, such as Mars, may also shed new lights on the outstanding questions regarding the formation of the continental crust on the Earth and the emergence of plate tectonics.

---

\* University of Toulouse, France

Last, but not least, these findings have also implications for the existence and nature mineralization processes at the surface of Mars and for the availability of metals at shallow depths. A large portion of ore deposits are associated on the Earth with differentiated rocks, whereas recent studies have mostly focused on Ni-Cu-PGE deposits associated with mafic rocks (Baumgartner et al. 2015). Evidence for continental crust should also prompt us to explore a wider range of processes and types of deposits, and their possible links to the crustal architecture.

Main collaborators: L. Baratoux, R. Baumgartner, M. Fall, M. Fiorentini, O. Gasnault, M. J. Jessell, A.S. André-Mayer, K. Kurita, M. Monnereau, P.M. Ndiaye, H. Samuel, M.J. Toplis, O. Vanderheaghe, M. Wieczorek,

## References

- Arndt, N. 2014. Formation and Evolution of the Continental Crust. *Geochemical Perspectives*, 2, 3, 405 – 530.
- Baratoux, D., Toplis, M.J., Monnereau, M., Gasnault, O. et al. 2011. Thermal history of Mars inferred from orbital geochemistry of volcanic provinces. doi:10.1038/nature09903
- Baratoux, D., M. J. Toplis, M. Monnereau, and V. Sautter. 2013. The petrological expression of early Mars volcanism, *J. Geophys. Res.: Planets*, 118, doi:10.1029/2012JE004234.
- Baratoux, D., H. Samuel, C. Michaut, M. J. Toplis, M. Monnereau, M. Wieczorek, R. Garcia, and K. Kurita (2014), Petrological constraints on the density of the Martian crust, *J. Geophys. Res. Planets*, 119, 1707-1727, doi:10.1002/2014JE004642.
- Baratoux et al. Crustal differentiation on Earth and Mars from Potassium and Thorium distributions. Submitted to *Nature Communications*.
- Carter, J., Poulet, F. 2013. Ancient plutonic processes on Mars inferred from the detection of possible anorthositic terrains. *Nature Geoscience*. doi:10.1038/NGEO1995.
- Filiberto, J., and R. Dasgupta. 2015. Constraints on the depth and thermal vigor of melting in the Martian mantle, *J. Geophys. Res. Planets*, 120, 109–122, doi:10.1002/2014JE004745.
- Grott et al. 2013. Long-Term Evolution of the Martian Crust-Mantle System. *Space Science Reviews*, 174, 49–111.
- Humayun et al. 2013. Origin and age of the earliest Martian crust from meteorite NWA 7533. doi:10.1038/nature12764.
- Sautter, V., et al. (2014), Igneous mineralogy at Bradbury Rise: The first ChemCam campaign at Gale crater, *J. Geophys. Res. Planets*, 119, doi:10.1002/2013JE004472.
- Sautter et al. 2015. In situ evidence for continental crust on early Mars. Doi:10.1038/NGEO2474.
- Wray et al. 2012. Prolonged magmatic activity on Mars inferred from the detection of felsic rocks. *Nature Geoscience*. doi:10.1038/NGEO1994.

## Crust–mantle interactions in hot orogens characterised by counterclockwise P–T–t paths and slow cooling

by

Michael Brown<sup>1</sup>, in collaboration with Fawna Korhonen<sup>2</sup>, Chris Clark<sup>3</sup>, John D. Foden<sup>4</sup>, and Richard Taylor<sup>3</sup>

Although the title is general, my comments will be based on a specific example from outside the Australian continent. Notwithstanding, the example provides useful insight into the dynamics of the continental lithosphere and its interaction with the asthenosphere that is useful in understanding the evolution of the Australian continent. The terms ‘counterclockwise’ (CCW) and ‘clockwise’ (CW) are used in petrology for pressure(P)–temperature(T)–time(t) paths described by rocks that record increasing P prior to and after the maximum T or decreasing P prior to and after the maximum T, respectively. For orogens characterised by CW P–T–t paths, granulite facies and ultrahigh temperature (UHT) metamorphic conditions were most likely generated during collisional orogenesis, particularly in long-lived plateaux with high internal concentrations of heat-producing elements and low erosion rates (Clark et al., 2011). By contrast, for orogens characterised by CCW P–T–t paths there is an unavoidable requirement for mantle heat to achieve extreme thermal conditions, which raises questions about mantle contamination of fugitive ‘crustal’ melts and cooling the crust.

Implicit in the peritectic assemblage entrainment hypothesis for the evolution of granite magma (Clemens et al., 2011; Clemens and Stevens, 2012), and its predecessor—restite unmixing (Chappell et al., 1987), is the concept of consanguinity between lower crustal granulites and upper crustal granites. However, for crust that evolves along CCW P–T–t paths, it is important to determine whether the production of granite magma in the lower crust was a closed-system process with respect to mass input from the mantle. This question is commonly addressed by inversion of geochemical data from upper crustal granites. However, a complementary approach is to assess the kinship among residual granulites and spatially associated granites in the exhumed deep crust of orogens to determine whether they are consanguineous or affinal.

As an example I take the Eastern Ghats Province (EGP) of India, part of a large long-lived Grenville-age UHT orogen characterized by a CCW evolution and peak temperature of ~950–1000°C at pressures of ~0.6–0.8 GPa (Korhonen et al., 2013a, 2013b, 2014). Here granite is interleaved with residual sillimanite–garnet or orthopyroxene–garnet granulites (Korhonen et al., 2015); zircon and monazite geochronology demonstrates contemporaneity and indicates slow rates of cooling (~1°C/Ma). Within the central part of the UHT province, geochemical data, in particular the Nd and Sr isotope compositions of the granites may be matched by simple mixing among the various granulites, suggesting that the granites may be consanguineous with these residual rocks. However, by including geochemical data available from an adjacent area to the north, it becomes clear that an increasingly important mass input from the mantle was involved in traversing from southwest to northeast, as confirmed by modeling assimilation–fractional crystallization between an exemplar mantle-derived melt at 1,000 Ma and the range of residual crustal lithologies (Korhonen et al., 2015).

It is difficult to cool hot crust slowly. Therefore, this feature provides a tight constraint on the processes by which such crust could have formed. Cooling over timescales >100 Ma implies that conductive transfer of heat occurred over vertical distances that were greater than the thickness of normal continental crust and strongly suggests that both crust and mantle were involved in the process (Oxburgh, 1990). In the EGP, the regional extent of UHT conditions requires an incursion of heat from the mantle and the metamorphic evolution of thickening after heating followed by slow cooling suggests an extended lithosphere that relaxed thermally to its former thickness. Whole lithosphere extension and mantle magmatism are strongly coupled because both perturb the thermal structure of the lithosphere and extension favors vertical transport of mantle melts. In such a dynamic environment, the spatial variation in mantle contribution to the granites is likely related to the changing feedback between rates of extension and mantle melt flux from southwest to northeast (cf. Karakas and Dufek, 2015), leading to a change in the granulite–granite relationship from consanguineous to affinal. In conclusion, in the EGP whole lithosphere extension, under conditions of higher mantle temperature and crustal heat production at 1,000 Ma, increasing mantle input from southwest to

1 Laboratory for Crustal Petrology, Department of Geology, University of Maryland, College Park, MD 20742 USA

2 Geological Survey of Western Australia, East Perth WA 6004, Australia

3 Department of Applied Geology, Curtin University, Perth WA 6845, Australia

4 Earth Sciences, Faculty of Sciences, University of Adelaide, SA 5005, Australia

northeast, melt transfer from lower to upper crust, and thermal relaxation were the dominant mechanisms by which the CCW UHT granulites and associated granite remnants were generated and slowly cooled.

## References

- Clark, C., Fitzsimons, I.C.W., Healy, D. and Harley, S.L., 2011. How does the continental crust get really hot? *Elements*, 7, 235–240.
- Clemens, J. D., Stevens, G. and Farina, F., 2011. The enigmatic sources of I-type granites: The peritectic connexion. *Lithos*, 126, 174–181.
- Clemens, J.D. and Stevens G., 2012. What controls chemical variation in granitic magmas? *Lithos*, 134–135, 317–329.
- Chappell, B.W., White, A.J.R. and Wyborn, D. The importance of residual source material (restite) in granite petrogenesis. *Journal of Petrology*, 28, 1111–1138.
- Karakas, O. and Dufek, J., 2015. Melt evolution and residence in expanding crust: Thermal modeling of the crust and crustal magmas. *Earth and Planetary Science Letters*, 425, 131–144.
- Korhonen, F.J., Brown, M., Clark, C. and Bhattacharya, S., 2013a. Osumilite-bearing equilibria and implications for the evolution of the Eastern Ghats Province, India. *Journal of Metamorphic Geology*, 31, 881–907.
- Korhonen, F., Brown, M., Clark, C., Foden, J.D. and Taylor, R., 2015. Are granites and granulites consanguineous? *Geology*, 43, doi:10.1130/G37164.1
- Korhonen, F.J., Clark, C., Brown, M., Bhattacharya, S. and Taylor, R., 2013b. How long-lived is ultrahigh temperature (UHT) metamorphism? Constraints from zircon and monazite geochronology in the Eastern Ghats orogenic belt, India. *Precambrian Research*, 234, 322–350.
- Korhonen, F.J., Clark, C., Brown, M. and Taylor, R., 2014. Taking the temperature of Earth's hottest crust. *Earth and Planetary Science Letters*, 408, 341–354.
- Oxburgh, E.R., 1990. Some thermal aspects of granulite history. In: *Granulites and Crustal Evolution*. (eds Vielzeuf, D. & Vidal, Ph.), pp. 569–580, Kluwer Academic Publishers, The Netherlands.

# Transport of metals in hydrothermal fluids

by

Joël Brugger<sup>1</sup>, Barbara Etschmann<sup>1</sup>, Yuan Mei<sup>1,2</sup>, Weihua Liu<sup>2</sup>

The hydration and complexation of metals in hydrothermal fluids are key processes controlling the mobility of elements in the Earth's crust, leading for example to the formation of ore deposits from which the World's supply of Fe, Mn, Ag, Au, Pd, Cu, Zn, Co, Pb, U, Mo is mined. In the past 20 years a large amount of in situ spectroscopic data complemented by increasingly accurate first principle molecular dynamic simulations have dramatically improved our understanding of the nature and geometry of the metal complexes that are responsible for metal transport in the upper crust. This new information underpins a "Coordination Chemistry" approach to ore transport and deposition. We present a Periodic Table of Metals Coordination Chemistry in Hydrothermal Fluids based on a review of the literature to illustrate the unifying principles brought upon by the concepts of coordination chemistry. We show that the different coordination geometries (e.g., linear versus tetrahedral versus octahedral) of metal complexes control some of the first order behaviours of these metals in hydrothermal systems, such as their relative affinity for low-density, vapour-like fluids. For some elements, fractionation and solubility gradients are associated with changes in coordination geometry brought upon by changes in pressure, temperature, and ligand availability (activity). For example, the differential mobility of Zr in aqueous fluids and hydrated melts in subduction environments was related to changes in coordination geometry in different media. Such coordination changes also affect metal ratios in hydrothermal fluids, including the ratios of geochemical pairs such as Zn/Cd, Fe/Mn, and Co/Ni. This molecular-level of understanding of metal speciation also underpins the development of more accurate models of reactive transport over wide ranges in pressure, temperature, fluid composition, and physical states. In particular, changes in coordination geometry are associated with large changes in entropy; hence coordination changes usually occur rapidly as a function of temperature (few 10's of °C), and need to be taken into account for extrapolating the thermodynamic properties of metal complexes.

## References

- Chase, M.W., NIST-JANAF Thermochemical Tables. J. Phys. Chem. Ref. Data, Monograph No.9. 1998. 1961.
- Clark, C., B. Grguric, and A.S. Mumm, Genetic implications of pyrite chemistry from the Palaeoproterozoic Olary Domain and overlying Neoproterozoic Adelaidean sequences, northeastern South Australia. *Ore Geology Reviews*, 2004. 25(3-4): p. 237-257.
- Klein, F. and W. Bach, Fe-Ni-Co-O-S Phase Relations in Peridotite-Seawater Interactions. *Journal of Petrology*, 2009. 50(1): p. 37-59.
- Robie, R.A. and B.S. Hemingway, Thermodynamic properties of minerals and related substances at 298.15 K and 1 bar (105 Pascals) pressure and higher temperatures. U.S. Geological Survey Bulletin, 1995. 2131.
- Shvarov, Y. and E. Bastrakov, HCh: a software package for geochemical modelling. User's guide. AGSO record, 1999. 1999/25: p. 60 pp.

1. School of Earth, Atmosphere and the Environment, Monash University, Clayton Victoria 3800

2. CSIRO Mineral Resources Flagship, Clayton Victoria 3168

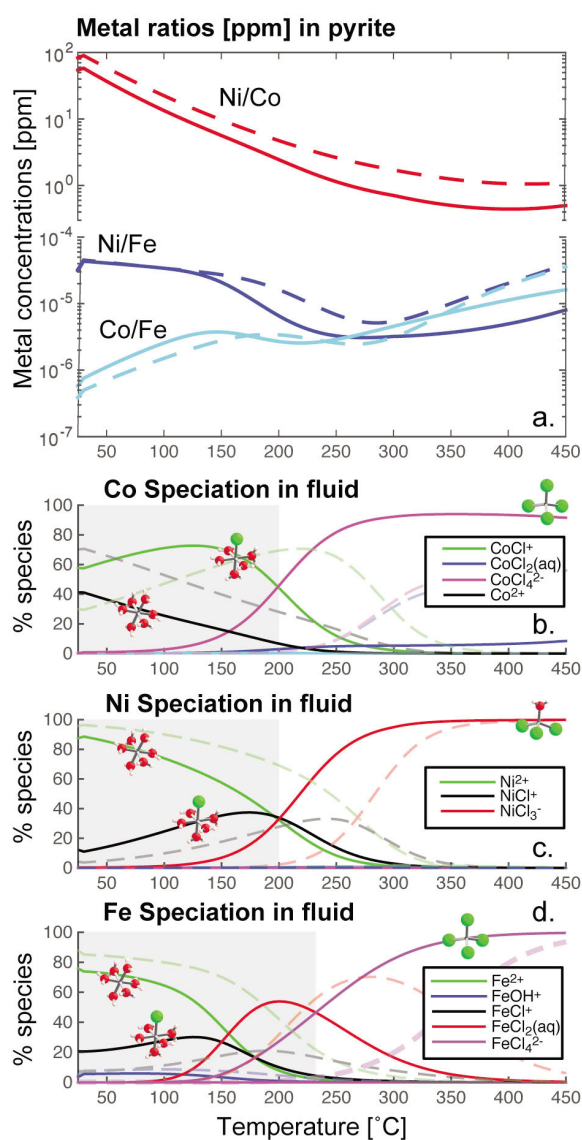


**Figure.** Calculations of Ni, Co and Fe speciation and solubility in a pyrite-hematite-magnetite assemblage, in solutions with 0.6 m NaCl (~seawater; solid lines) and 3 m NaCl (dashed lines). The pyrite is set to contain 1000 ppm Co and 1000 ppm Ni (Clark et.al, 2004). Pyrite, cattierite and vaesite are assumed to form an ideal solid solution. Calculations were conducted using the HCh software (Shvarov and Basrtakov, 1999), assuming ideal solid solution behaviour among pyrite, vaesite, and cattierite. Sources of thermodynamic properties: cattierite, (Robie and Hemingway, 1995); vaesite, Gibbs free energy and entropy as in Klein and Bach2009), and heat capacity from (Chase, 1998).

# Australian Architecture Reference Model (AusARM): Towards constraining the spatial and temporal evolution of the lithosphere

by

Karol Czarnota<sup>1</sup>, Nicky White<sup>2</sup>, Michael Doublier<sup>1</sup>, Jingming Duan<sup>1</sup>, Malcolm Nicoll<sup>1</sup>,  
and Alexei Gorbatov<sup>1</sup>

The emerging economic imperative to improve resource exploration undercover and the unabating desire to understand deep Earth processes has resulted in a bloom of continental scale datasets and models pertinent to the study of the Australia lithosphere. Geoscience Australia, as the national geoscience data custodian, has fostered much of this activity and is working towards an Australian Architecture Reference Model (AusARM) which seeks to integrate disparate datasets and models, making them accessible through the recently redeveloped EarthSci 3D viewer (<https://github.com/GeoscienceAustralia/earthsci>). Current efforts are focused on compiling and updating major surfaces through, and petrophysical properties of, the Australian lithosphere with the aim not only to constrain the present lithospheric architecture but also its temporal evolution.

Major surface mapping activities include a sustained initiative to map chrono-stratigraphically defined basin boundaries to update OZ SEEBASE (de Vries et al., 2006), compile constraints on the Moho (Salmon et al., 2013), the lithosphere-asthenosphere boundary (e.g. Czarnota et al., 2014) and the maximum base of magnetisation (Chopping and Kennett, 2015). The distribution of major crustal boundaries interpreted by Korsch and Doublier (2015) on the basis of deep reflection seismic profiles and ever-growing potential field data (<https://www.ga.gov.au/gadds>) is being extended in 3D. In order to manage this data a publicly accessible database to store and maintain point Estimates of these Geological and Geophysical Surfaces (EGGS) is currently being developed and populated.

Volumetrically, the intention is to provide a national coverage of velocity, density and conductivity of the Australian Plate. Currently, the Australian Seismological Reference Model (AuSREM) (Kennett et al., 2013; Salmon et al., 2013) provides the best constraints on the velocity structure of the Australian Plate. To further refine this coverage we are undertaking joint bulk-sound and shear tomography along with P and S tomography following Gorbatov and Kennett (2003) utilising data from permanent and temporary seismometer deployments and

the GA earthquake catalogue. Subsequently we intend to utilise these results to refine national density models. A national model of conductivity has been produced by Wang et al. (2014) based on data from 57 stations from the Australia-wide Array of Geomagnetic Stations. Increased conductivity resolution will be provided by the ambitious Australian Lithospheric Architecture Magnetotelluric Project (AusLAMP) which aims to deploy long-period magnetotelluric stations across the Australian continent at a nominal resolution of  $0.5^\circ \times 0.5^\circ$ . AusLAMP data collection and modelling is complete over Victoria (Duan et al., in prep) and well underway over South Australia.

In addition there is an ongoing program of national chronostratigraphic solid geology, metamorphic and radioactive isotope mapping along with selected lithological compilations which place important constraints on the temporal evolution of the lithosphere. Solid geological interpretation has started by stripping Cenozoic cover. National metamorphic grade maps are being compiled based on available information from literature. A national coverage of Sm-Nd isotopes exists (Champion, 2013), a national compilation of Pb isotopes has commenced with south eastern Australia (Huston et al., in press) and a national database of Lu-Hf isotope data is under construction. Building on the national synthesis of mafic and ultramafic magmatic events by Thorne et al. (2014) a focused program on the spatial distribution and geochemistry of alkaline rocks is underway.

is required to be thick and depleted by  $50\text{--}70 \text{ kg m}^{-3}$ . The actual state of depletion has been assessed by adopting Tainton and McKenzie (1994) modelling of REE concentrations of diamond bearing ~20 Ma lamproites (Evans et al., 2013) which intrude into the FT reveal that the base of the lithospheric mantle is indeed thick and depleted within the expected density range. Four conclusions arise. First, the lithosphere beneath the western Canning Basin in the Ordovician and now has a standard thickness of (~120 km), whereas the FT was underlain by thick (>200 km) lithosphere which has thinned to no less than ~120 km thick. Secondly, the discrepancy between estimates of lithospheric thickness derived from subsidence data in the Western Canning and shear wave tomography suggests that the latter technique is currently not resolving lithospheric thickness variations on < 300 km half wavelengths. Similarly in the Yilgarn major isotopic and geological domains (e.g. Murchison

1 Geoscience Australia, GPO Box 378, Canberra, ACT 2601, Australia,

2 Bullard Laboratories, University of Cambridge, Cambridge CB3 0EZ, UK

juvenile corridor < 250 km wide) are not expressed within existing seismic tomography models. Thirdly, variations in lithosphere thickness beneath the Canning suggest the boundary between the North Australia and Western Australia Cratons is likely to be on the western side of the FT. Last, integration of AusARM datasets over the FT provides a fundamental insight into lithosphere evolution, indicating that thinning of thick lithosphere to thicknesses > 120 km is thermally stable and is not accompanied by re-thickening of the lithospheric mantle as suggested by established models.

## References

- Champion, D. C., Neodymium depleted mantle model age map of australia explanatory notes and user guide, Geoscience Australia, Record 2013/44, 209, doi:10.11636/Record.2013.044, 2013.
- Chopping, R., and B. L. N. Kennett, Maximum depth of magnetisation of australia, its uncertainty, and implications for curie depth, *GeoResJ*, 7, 70–77, doi:10.1016/j.grj.2015.06.003, 2015.
- Crosby, A. G., S. Fishwick, and N. White, Structure and evolution of the intracratonic Congo Basin, *Geochem. Geophys. Geosy.*, 11, 1–20, doi:10.1029/2009gc003014, 2010.
- Czarnota, K., G. G. Roberts, N. J. White, and S. Fishwick, Spatial and temporal patterns of australian dynamic topography from river profile modeling, *J. Geophys. Res.-Sol. Ea.*, 119 (2), 1384–1424, doi:10.1002/2013JB010436, 2014.
- de Vries, S., N. Fry, and L. Pryer, OZ SEEBASE Proterozoic Basins, Tech. rep., FROG TECH, 2006. Duan, J., et al., Illuminating Victoria's lithosphere conductivity structure: AusLAMP, in prep.
- Evans, N. J., B. A. McInnes, B. McDonald, M. Daniš'ík, F. Jourdan, C. Mayers, E. Thern, and D. Corbett, Emplacement age and thermal footprint of the diamondiferous Ellendale E9 lamproite pipe, Western Australia, *Miner. Deposita*, 48, 413–421, doi:10.1007/s00126-012-0430-7, 2013.
- Gorbatov, A., and B. L. N. Kennett, Joint bulk-sound and shear tomography for western pacific subduction zones, *Earth Planet. Sci. Lett.*, 210 (3–4), 527–543, doi:10.1016/S0012-821X(03)00165-1, 2003.
- Huston, D. L., D. C. Champion, T. P. Mernagh, P. M. Downes, P. Jones, G. Carr, D. Forster, and V. David, Metallogensis and geodynamics of the lachlan orogen: New (and old) insights from spatial and temporal variations in lead isotopes, *Ore Geology Reviews*, doi:10.1016/j.oregeorev.2015.07.005, in press.
- Kennett, B. L. N., A. Fichtner, S. Fishwick, and K. Yoshizawa, Australian Seismological Reference Model (AuSREM): mantle component, *Geophys. J. Int.*, 192 (2), 871–887, doi:10.1093/gji/ggs065, 2013.
- Korsch, R. J., and M. P. Doublier, Major crustal boundaries of australia, 2nd edition, doi: 10.4225/25/555C181CC0EAE, 2015.
- Salmon, M., B. L. N. Kennett, and E. Saygin, Australian Seismological Reference Model (AuSREM): crustal component, *Geophys. J. Int.*, 192 (1), 190–206, doi:10.1093/gji/ggs004, 2013.
- Tainton, K. M., and D. McKenzie, The generation of kimberlites, lamproites, and their source rocks, *J. Petrol.*, 35 (3), 787–817, doi:10.1093/petrology/35.3.787, 1994.
- Thorne, J., M. Cooper, and J. C. Claoue-Long, Guide to using the australian mafic-ultramafic magmatic events gis dataset : Archean, proterozoic and phanerozoic magmatic events, Geoscience Australia, Record 2014/39, 103, doi:10.11636/Record.2014.039, 2014.
- Wang, L., A. P. Hitchman, Y. Ogawa, W. Siripunvaraporn, M. Ichiki, and K. Fuji-ta, A 3-d conductivity model of the australian continent using observatory and magnetometer array data, *Geophysical Journal International*, 198 (2), 1171–1186, doi:10.1093/gji/ggu1

## Geophysical Detection of Mineral Systems in the Deep Crust and Upper Mantle

by

Mike Dentith\*

The emergence of the mineral systems paradigm as a framework for assessing prospectivity at the regional scale and/or under cover has resulted in increased interest in geophysical methods capable of resolving features in the deep crust and lithospheric mantle. For several important mineral systems, key prospectivity criteria are the presence of deep penetrating faults (which acted as conduits for fluids sourced in the mantle) and anomalous zones of mantle and/or crust (indicative of fluid source regions). For technical and financial reasons teleseismic seismic and electromagnetic geophysical methods are the preferred means of detecting such features.

Magnetotellurics (MT) is a passive, frequency domain, form of electromagnetic surveying. The frequency-dependent depth penetration of natural electromagnetic fields is exploited to map variations in electrical conductivity in the sub-surface. Depending on local conditions, deployment of equipment for several days allows conductivity variations through the entire lithosphere to be mapped. MT is increasingly used for regional-scale prospectivity analysis-related studies and been demonstrated to be an effective means of mapping (palaeo-)cratonic boundaries and major faults. Variations in conductivity detected in the mantle may be indicative of regions of metasomatism/melting. Conductive zones in the deep crust under major IOCG deposits have also been recorded in South Australia, suggesting the method can be used for exploration targeting in the initial stages of exploration. The main drawbacks with the MT method are the computationally intensive inverse modelling methods required to create 3D conductivity models, the poor resolution and ambiguity of the results and, in particular, the generally poor understanding of the causes of electrical conductivity variations in the deep crust.

The highest resolution geophysical method for studying the deep crust is the seismic reflection method. Capable of resolving features with dimensions of hundreds of metres in the lower crust, this method responds to changes in acoustic impedance (product of seismic velocity and

density). Although detailed images can be produced in this fashion, the high cost of the method limits its use in general and to only 2D survey geometries. The complex geology of many mineralised terrains, often combined with necessary but non-ideal survey geometries, means the resulting data can be very difficult to interpret. Nevertheless deep seismic reflection surveys remain the most reliable means of mapping major faults and crustal boundaries in the deep crust.

Teleseismic surveys are a form of passive seismic surveys which derive the structure of the lithosphere underneath a survey station from recordings of distant earthquakes. Conversions and reverberations of different types of seismic waves allow velocity variations in the region below the station to be determined. This is referred to as the 'receiver function'. Because the recording equipment is relatively simple surveying is cheap. The major limitation is that a sufficient number of suitable earthquakes need to be recorded during a deployment. Typically deployments of at least several months are required to ensure this condition is likely to be satisfied. Established teleseismic methods map major velocity boundaries such as the Moho, but emerging techniques based on arrays of recorders and common-conversion-point (CCP) processing of these data allow cross-section-like presentations of crustal structure. A comparison of such a dataset, from the Capricorn Orogen in Western Australia, with a coincident deep seismic reflection profile suggests that major structures and crustal domains with different seismic properties can be mapped in this fashion.

Although ideally terrain-scale prospectivity is assessed based on a network of deep seismic reflection profiles, in practice this is prohibitively expensive. A practical alternative is to use a limited amount of seismic reflection data as a 'geological control' and use networks of MT and teleseismic traverses to extrapolate geological structure into adjacent regions.

---

\* Centre for Exploration Targeting/School of Earth & environment, The University of Western Australia

# Sulfur and metal fertilization of the lower continental crust

by

**Marco Fiorentini<sup>1</sup>, Marek Locmelis<sup>2</sup>, John Adam<sup>3</sup>, Tracy Rushmer<sup>3</sup>, Federica Zaccarini<sup>4</sup>, Giorgio Garuti<sup>4</sup>,  
Zoja Vukmanovic<sup>5</sup>, Stefano Caruso<sup>1</sup>, Marilena Moroni<sup>6</sup>, Steve Barnes<sup>7</sup>, Steve Reddy<sup>5</sup>, Belinda Godel<sup>7</sup>**

Early Permian pipe-like bodies of amphibole- and sulphide-rich peridotite were emplaced into the crust-mantle section of the Ivrea-Verbano Zone of northwest Italy. In this study, we investigated one such body, the Valmaggia pipe, and we used an integrated approach to unravel the relationship between the microstructural features of the pipe, its 3D mineralogical and mineralogical-chemical textural network and its emplacement mechanism at the interface between the lithospheric mantle and the base of the continental crust. The outcomes from this work bear an insight on the capacity of hydrous mafic melts to transport sulfur and chalcophile metals from the mantle into the crust. We propose that the pipe rocks and their sulfide mineralisation are cumulates that crystallized under lower crustal conditions ( $\leq 0.8$  GPa) within feeder conduits for ascending basaltic magmas. The original cumulates were dunitic, but during cooling of the magmatic system these partially reacted with water-rich melts (at 1000–1050 °C) to produce abundant amphibole and (lesser) orthopyroxene, together with residual olivine. Plagioclase, mica, apatite and spinel either co-crystallized during this stage and/or precipitated during the final solidification of residual intercumulus liquid. The parent magmas of the pipes were probably alkaline and sodic (similar to alkali olivine basalt or basanite) and enriched in a broad range of incompatible elements. They display a signature that resembles that of high-Nb basalts, which are commonly associated with adakites in post-collisional settings worldwide. Results from EBSD analysis and 3D X-Ray tomographic studies on cumulate minerals from the Valmaggia pipe suggest that deformation of olivine, amphibole and orthopyroxene occurred synchronously during emplacement of the magma. In terms of multiple sulfur isotope systematics, the mineralization associated with the pipes generally displays a mantle-like  $\delta^{34}\text{S}$

signature ( $0\pm 2\text{‰}$ ), with rare but notable lighter signatures ( $\delta^{34}\text{S} = -4\text{‰}$ ). The results from the 3D X-Ray tomographic study together with the grain and size analysis support the hypothesis that the parental magma to the Valmaggia pipe was sulfide saturated at the time of emplacement. In the initial stages of magma emplacement, fine sulfide blebs (made up of mainly pyrrhotite and minor amounts of chalcopyrite) were transported and subsequently incorporated into the early crystallising olivine cumulates. Subsequently, larger blebs formed due to coalescence of the finer ones along the margins of the pipe, where shear flow and wall rock interactions favoured the accumulation of Ni-Cu-PGE sulfide mineralisation. Sulfide transport and coalescence may have also been favoured by the exsolution of  $\text{CO}_2$ -bearing supercritical liquids. Deep-seated magmatic mineral systems such as the ones exposed in the Ivrea Zone provide fundamental insights into the nature of volatile and metal transfer from the lithospheric mantle into the base of the continental crust.

- 
- 1 CET/CCFS, The University of Western Australia, Crawley, Australia
  - 2 NASA Goddard Space Flight Center, Greenbelt, MD 20771, USA
  - 3 Macquarie University/CCFS, North Ryde, Australia;
  - 4 Department of Applied Geosciences and Geophysics, University of Leoben, Austria
  - 5 Curtin University/CCFS, Perth, Australia
  - 6 Earth Science Department, Università degli Studi di Milano, Italy
  - 7 CSIRO Mineral Resources Flagship, Perth, WA.

## Evolution of the lithospheric mantle by melt/rock interaction and its effects on the composition of lithosphere-derived volcanic melts

by

Stephen Foley\*

The first main phase of stabilization of the continental mantle lithosphere appears to have taken place at 3.5 – 3.0 Ga. This means that some parts of the cratonic mantle lithosphere have had three-quarters of Earth history to further evolve after their stabilization.

At the time of its formation, it is likely that a large proportion of the cratonic lithosphere was considerably more depleted in melt components than it is now, indeed it is probable that much of the present unsampled lower cratonic lithosphere, i.e. the parts located away from the sites of surface volcanism, are still in a geochemically very depleted state. It is now recognized that the introduction of melts into the lower lithosphere causes mantle metasomatism, and that this process leads to oxidation of the lower lithosphere, a process which is concentrated around the sites of later eruptions.

The evolution of the lower lithosphere by the introduction of melts depends on the types of melts that are introduced. These are likely to be dominated by melt types that hardly ever reach the surface, but are strongly enriched in volatile components such as H<sub>2</sub>O and CO<sub>2</sub>, and, in most cases, solidify completely within the lower lithosphere. They do not correspond to any of the common magma types that can be found as volcanoes or intrusions at or close to the surface. The reason for this difference is the effect of the volatile components on melting of mantle peridotite: small amounts of volatiles can depress the melting point of peridotite by hundreds of degrees at pressures corresponding to the lower half of the cratonic lithosphere. The exact amount of solidus depression depends on the depth and the mixture of volatiles. Experiments have shown that a mixture of H<sub>2</sub>O and CO<sub>2</sub> will have a stronger effect than H<sub>2</sub>O alone, and that the solidus depression by mixtures of H<sub>2</sub>O and CH<sub>4</sub>, which exist in reduced conditions, will vary greatly depending on the activity of water in the mixture, but will generally be much less marked than that caused by H<sub>2</sub>O+CO<sub>2</sub> mixtures.

In summary, an incipient melting regime exists over a considerable temperature range before major melting begins. It is major melting that produces the voluminous melts commonly seen at the Earth's surface: at lower

degrees of melting, the low-volume intra-mantle melts are dominated by melts akin to carbonatites and carbonate-rich ultramafic lamprophyres (aillikites), which only very rarely occur at the surface. They are most commonly found in unusual geodynamic situations in which a craton has been split apart by later rifting events. This is indicated by the occurrence of these melts associated with the rifts and with the edges of cratons.

The oldest known carbonatites are around 3 Ga, whereas other alkaline rock types enriched in potassium first occur later: shoshonites and alkaline lamprophyres aged 2.7 Ga are known, followed by ultramafic lamprophyres at 1.9 Ga, kimberlites at 1.6 Ga, and lamproites chime in at 1.4 Ga. Although the low preservation potential of such rare rock types can never be discounted as a factor, it is most likely that this age progression indicates that the necessary conditions of formation were lacking before these times, meaning it is not that earlier ones have not been preserved, but that they could not be formed.

In the case of carbonatitic melts, this may be related to two factors; firstly the oxidation state, and secondly, the availability of sufficient concentrations of carbon for the production of batches of melts voluminous enough to reach the surface without solidifying. Both can be explained by the gradual oxidation of the mantle by metasomatism. As mentioned above, the early cratonic lithosphere was more depleted, and has been enriched and oxidized by successive metasomatic events. Carbonatites now occur most commonly in continental rifts, and the necessary concentration of CO<sub>2</sub> in these areas may be due to the accumulation of solid carbon (diamond) in the lower lithosphere over time, which is then rejuvenated in the form of CO<sub>2</sub> and consequently carbonate melts during redox melting when the rifting occurs.

The later occurrence of potassic melts is due to a similar phenomenon to this concentration of carbon in the sources of carbonatites, but in this case it is the pre-concentration of other elements. Potassic melts cannot be generated from peridotite by any reasonable (i.e. extractable) degree of melting. Instead they require pre-conditioning of the source by enrichment in these components, which means the solidification of one or more generations of earlier water-rich silicate melts. This requires time before sufficient pre-conditioning has occurred, as the metasomatic enrichments are likely to be episodic and not continuous, depending on large-

---

\* Macquarie University, Earth and Planetary Sciences, ARC Centre of Excellence for Core to Crust Fluid Systems

scale geodynamic movements. The earlier occurrence of shoshonitic rocks types (latest Archean) may be explained by their generation requiring the conjunction of water-rich melting conditions and pre-conditioning of the source with potassium and other incompatible elements, but not necessarily oxidizing conditions. Carbonate-rich ultramafic lamprophyres are restricted to later periods because they additionally require oxidizing conditions for the stabilization of carbonate.

In summary, the type of melt infiltration that the lower lithosphere has experienced has changed with time, and so the variety of melts produced on the modern Earth depends on the type, age, and severity of enrichment of the source, as well as the mechanism by which melting occurs.

## Constraints on kimberlite ascent mechanisms revealed by phlogopite compositions in kimberlites and mantle xenoliths

by

**Andrea Giuliani<sup>1,2</sup>, David Phillips<sup>2</sup>, Vadim S Kamenetsky<sup>3</sup>, Karsten Goemann<sup>4</sup>**

Kimberlite magmas are of economic and scientific importance because they represent the major host to diamonds and are probably the deepest magmas from continental regions. In addition, kimberlite magmas transport abundant mantle and crustal xenoliths, thus providing fundamental information on the composition of the sub-continental lithosphere. Despite their importance, the composition and ascent mechanism(s) of kimberlite melts remain poorly constrained. Phlogopite is one of the few minerals that preserves a history of fluid migration and magmatism in the mantle and crust and is therefore an invaluable petrogenetic indicator of kimberlite magma evolution.

Here we present major and trace element compositional data for phlogopite from the Bultfontein kimberlite (Kimberley, South Africa; i.e. the kimberlite type-locality) and from entrained mantle xenoliths. Phlogopite macrocrysts (~> 0.3-0.5 mm) and microcrysts (between ~0.1-0.3 mm) in the Bultfontein kimberlite display concentric compositional zoning patterns. The cores of these phlogopite grains exhibit compositions typical of phlogopite contained in peridotite mantle xenoliths. However, the rims of some grains exhibit compositions analogous to kimberlite groundmass phlogopite (i.e., high Ti, Al and Ba; low Cr), whereas other rims and intermediate zones (between cores and rims) exhibit unusually elevated Cr and lower Al and Ba concentrations. The latter compositions are indistinguishable from matrix phlogopite in polymict breccia xenoliths (considered to represent failed kimberlite intrusions) and from Ti-rich overgrowth rims on phlogopite in other mantle xenoliths. Consequently, it is likely that these phlogopite grains crystallized from kimberlite melts and that the high Ti-Cr zones originated from earlier kimberlite melts at mantle depths.

We postulate that successive pulses of ascending kimberlite magma progressively metasomatised the conduit along which later kimberlite pulses ascended, producing progressively decreasing interaction with the surrounding mantle rocks. In our view, these processes represent the fundamental mechanism of kimberlite magma ascent. Our study also indicates that, in addition to xenoliths/xenocrysts and magmatic phases, kimberlite rocks incorporate material crystallized at various mantle depths by previous.

- 
- 1 ARC Centre of Excellence for Core to Crust Fluid Systems and GEMOC, Department of Earth and Planetary Sciences, Macquarie University, North Ryde, 2019 NSW, Australia
  - 2 School of Earth Sciences, The University of Melbourne, Parkville, 3010 Victoria, Australia
  - 3 School of Physical Sciences, University of Tasmania, Hobart, 7001 Tasmania, Australia
  - 4 Central Science Laboratory, University of Tasmania, Hobart, 7001 Tasmania, Australia

# Neutral-Buoyancy Rule Over-Ruled: Crustal Underplating by Buoyant Magmas during Orogeny

by

Robert R Loucks

Magma bodies ascend from their melt source due to lower density than the surrounding rock. A traditional and still commonly expressed viewpoint is that ascending magmas stall at a neutral buoyancy level, at which point the average density of the magma body matches the average density of the surrounding rock over the depth interval spanned by the magma column. Several lines of evidence demonstrate that magmas ascending via subvertical feeder dykes commonly stall and produce sub-horizontal intrusions within denser country rock: (1) The common occurrence of substantial negative gravity anomalies associated with igneous intrusions demonstrates that the neutral buoyancy hypothesis is commonly inapplicable (Vigneresse & Clemens, 2000). (2) Seismic detection (blocked S waves; high  $V_p/V_s$  ratios) of subhorizontal magma chambers near at or just beneath the Moho has been reported in Kamchatka, Hawaii, the Canary Islands and elsewhere. (3) Cognate xenoliths of ultramafic and mafic cumulates and phenocrysts that crystallised at uppermost mantle pressures occur in andesitic and dacitic lavas in the Aleutian, Western Luzon, Lesser Antilles and other arcs, indicating that mantle-derived basaltic magmas stalled near the Moho and crystallised to advanced stages of magmatic differentiation before erupting. (4) Where the roots of magmatic arcs are exposed at various localities around the world, lower-crustal layered ultramafic-mafic cumulate complexes tens of km in horizontal dimension provide evidence of hydrous arc magma sheets stalling and crystallising for long periods at Moho depths under dense roof rocks. Thybo & Artemieva (2013) review seismic evidence of mafic-ultramafic intrusions that have locally underplated the crust at or near the Moho in intra-plate and plate-margin settings, but they do not discuss the mechanics of magmatic underplating of the crust. Hydrous basaltic arc magmas are extremely buoyant relative to lithospheric mantle ultramafic lithologies and are also buoyant with respect to mafic lower crust that is composed mainly of gabbroid and mafic granulite lithologies.

Lithospheric mantle and lower-crustal rocks that deform viscously on long time scales and that generally cannot accumulate tectonically imposed elastic stress to generate

earthquakes are susceptible to elastic failure on the short time scales of hydraulic fracturing to emplace dykes and sills. Menand et al (2010) report laboratory analogue experiments in which a buoyant fluid-filled hydraulic fracture rotates from a subvertical dyke to a subhorizontal sill within a surrounding gelatin medium having homogeneous density but upward-increasing viscosity and upward increase in horizontal compressive stress imposed remotely at the margins of the experimental tank. That experimental demonstration of stress entrapment of buoyant fluid seems relevant to explaining the development of magma chambers within the uppermost lithospheric mantle in orogenically deforming compressive segments of the central Aleutian arc under Adak volcano, and in the Western Luzon arc under Mt. Pinatubo. In those cases, the magma chambers are fed by hydrous basaltic melts from the deeper mantle; after magmatic differentiation by precipitation of ultramafic-mafic crystal cumulates, residual adakitic magmas having greater buoyancy erupt with entrained high-pressure xenoliths and high-pressure phenocryst assemblages.

Central Kamchatka is undergoing orogeny where it is over-riding the subducting western Aleutian arc. In the deformation zone, the Klyuchevskoy cluster of stratovolcanoes erupts basalts and mafic andesites fed from a seismically imaged magma chamber just beneath the Moho (Levin et al., 2014). Deep seismic sounding studies using surface explosions detected multiple reflecting boundaries in the 25–45 km depth range, which represent a complex and gradual crust-mantle transition interval occupied by sills of mafic and ultramafic cumulates. Seismicity to 60 km depth under the Klyuchevskoy group represents brittle-elastic fracture of the uppermost mantle, associable with melt migration by hydraulic fracturing (Levin et al., 2014). Gorelchik et al. (1997) report seismic evidence (blocked S waves) of a magma chamber or stacked series of magma chambers directly beneath Sheveluch volcano (~80 km NE of Klyuchevskoy) spanning the 10–30 km depth interval and straddling the Moho at ~25 km depth. They report that seismicity due to hydraulic fracturing in the mantle at 120–90 km depth precedes major eruptions of Sheveluch; this suggests that adakitic andesitic emanations from the Moho-level and crustal magma chamber(s) are triggered by injections of mantle-derived basaltic magma.

---

\* Centre for Exploration Targeting/School of Earth & environment, The University of Western Australia

Compressive deformation within magmatic arcs commonly occurs (1) at indentations within the over-riding plate, such as oroclinal bends (e.g., the Arica orocline in the central Andes, or the southern Alaska orocline) or at cusp-like junctions of island arcs, at which tangential drag of the forearc has opposing senses of motion that converge at the junction; and (2) where buoyant topographic highs in the subducting plate drag along the base of the over-riding plate causing lithospheric shortening. Volcanic gaps commonly occur within orogenically deforming arc segments beneath which subduction continues and magma generation presumably continues (McGeary et al, 1985). Adakitic andesites and dacites commonly occur at the edges of such volcanic gaps, and are the earliest magmas to appear upon resumption of volcanism within the gaps, as compressive stress is relieved by geodynamic re-arrangements.

Arc magmatism within compressive arc segments has distinctive geochemical trends over the mafic-to-felsic range of magmatic differentiation that seem to be unique to such stress regimes: relatively flat trends of whole-rock Zr vs  $\text{SiO}_2$  and nearly constant Sr/Zr with increasing  $\text{SiO}_2$ , whereas Zr rises strongly and Sr/Zr declines strongly with increasing  $\text{SiO}_2$  in non-compressive arc segments; and normalised whole-rock rare-earth element patterns of andesites, dacites and rhyolites generally decline strongly in the interval La to Dy or Ho and then rise to Lu, and lack a substantial dip at Eu, whereas andesites, dacites, and rhyolites from non-compressive arc segments have REE patterns are generally nearly flat but have a strong dip at Eu. These features in zircon-bearing igneous suites can be used to radiometrically date compressive episodes in ancient magmatic arcs.

Porphyry-type and high-sulfidation-type magmatic-hydrothermal copper-gold ore deposits are apparently restricted to arc segments that have experienced orogenic compressive stress during or immediately preceding the ore-forming magmatism.

## References

- Lyons, J.B., Campbell, J.G. & Erikson, J.P., 1996. Gravity signatures and the geometric configurations of some Oliverian plutons: Their relation to Acadian structures. *Geol. Soc. Am. Bull.* 108, 872–882.
- Vignerresse, J.-L. & Clemens, J.D., 2000. Granitic magma ascent and emplacement: neither diapirism nor neutral buoyancy, in Vendeville, B., Mart, Y. & Vignerresse, J.-L. (eds) *Salt, Shale and Igneous Diapirs in and around Europe*. Geological Society, London, Special Publications, 174, 1-19.
- Vignerresse, J.-L., Tikoff, B. & Améglio, L. 1999. Modification of the regional stress field by magma intrusion and formation of tabular granitic plutons. *Tectonophysics*, 302, 203-224.
- Thybo, H. & Artemieva, L.M., 2013, Moho and magmatic underplating in continental lithosphere. *Tectonophysics*, 609: 605-619.
- Menand, T., K. A. Daniels, and P. Benghiat (2010), Dyke propagation and sill formation in a compressive tectonic environment, *J. Geophys. Res.*, 115, B08201, doi:10.1029/2009JB006791.
- Levin, V, Droznina, S, Gavrilenko, M, Carr, M.J., & Senyukov, S, 2014, Seismically active subcrustal magma source of the Klyuchevskoy volcano in Kamchatka, Russia. *Geology*, 42: 983–986.
- McGeary, S., Nur, A. & Ben-Avraham, Z., 1985, Spatial gaps in arc volcanism: the effect of collision or subduction of oceanic plateaus. *Tectonophysics*, 119: 195-221.

# Magmatic gas reactions in sub-volcanic arcs

by

John Mavrogenes\*

Arc related ore deposits form by magmatic gas reactions with wall-rocks; at high pressures, porphyry deposits result while at lower pressures, “high sulfidation” deposits form. In this talk I use vein textures and mineral analyses to outline processes that lead to ore deposition. Experimental results are used to demonstrate how oxidised magmas and gases produce sulfide ores of widely differing character as a function of pressure.

## High-sulfidation Deposits

Vein gold deposits such as El Indio, Chile, formed in fracture arrays <1000 m beneath paleo-solfataras in volcanic terranes. Stable isotope data have confirmed a predominance of magmatic vapor during the deposition of arsenic-rich sulfide–sulfosalt assemblages in this deposit. These provide a unique opportunity to analyze the processes and products of high-temperature volcanic gas expansion in fractures that form the otherwise inaccessible infrastructure deep inside equivalent present-day fumaroles. Micro-analytical data for the wide range of heavy, semi-metals and metalloids (arsenic, antimony, bismuth, tin, silver, gold, tellurium and selenium) in the complex pyrite–enargite–Fe–tennantite assemblages from Copper Stage mineralization in the El Indio deposit document the progressive fractionation of sulfosalt melt that condensed from expanding vapor at about 15 MPa (150 bars) and >650°C. The sulfosalt melt aggressively corroded the earlier enargite and pyrite and hosts clusters of distinctive euhedral quartz crystals. The crystallizing sulfosalt melt also trapped an abundance of vugs within which heavy metal sulfide and sulfosalt crystals grew together with K–Al silicates and fluorapatite. These data and their geologic context suggest that, in high-temperature fumaroles on modern active volcanoes, over 90% of the arsenic content of the primary magmatic vapor (perhaps 2000 mg kg<sup>-1</sup>) was precipitated subsurface as sulfosalt. Subsurface fractionation may also account for the range of exotic Pb–Sn–Bi–Se sulfosalts observed in fumarole sublimates on active volcanoes such as Vulcano, Italy. Quartz microcrystals from El Indio preserve a rare glimpse into the high-temperature evolution of silica. Euhedral quartz microcrystals preserve cryptocrystalline cores that contain silica hydrates “opal” and moganite.

These phases are interpreted as metastable remnants of progressive dehydration from a precursor silica hydrate phase. Evidence for sequential dehydration from silica hydrate to quartz (silica hydrate–opal–moganite–quartz) is provided by SHRIMP <sup>18</sup>O microanalytical data that show oscillatory isotopic zoning from 3.6‰ to 16.2‰  $\delta^{18}\text{O}$  ( $\pm 0.5\text{‰}$ ) coupled with K and Al variations. The precursor silica hydrate was deposited between ~480–680 °C. Silica hydrate is metastable with respect to quartz and forms during rapid deposition of silica at high silica supersaturation, a consequence of rapid expansion of magmatic fluid into the fracture array that hosts the El Indio copper–gold deposit.

## Porphyry copper deposits

In porphyry deposits it is not clear that a single, copper-rich magmatic fluid could trigger both copper enrichment and the subsequent precipitation of sulfide ore minerals. By comparing observations of modern subduction zone volcanism with porphyry environments, an alternative process appears, in which copper enrichment initially involves metalliferous brines, that exsolve from large, intrusions assembled in the shallow crust over tens to hundreds of thousands of years. In a subsequent step, sulfide ore precipitation is triggered by the interaction of the accumulated brines with sulfur-rich gases, liberated in short-lived bursts from the underlying mafic magmas. High-temperature and high-pressure laboratory experiments to simulate such gas–brine interactions yield copper–iron sulfide minerals and hydrogen chloride gas at magmatic temperatures of 700–800 degrees C, with textural and chemical characteristics that resemble those in porphyry copper deposits (Blundy et al, 2015).

Subsequently, Henley et al (2015) showed that a very rapid chemisorption reaction occurs between sulfur dioxide gas, a principal component of magmatic gas mixtures, and calcic feldspar, an abundant mineral in the arc crust. The chemisorption reaction generates the mineral anhydrite and hydrogen sulfide gas, and triggers deposition of metal sulfides. This work suggested that SO<sub>2</sub> alone may trigger deposition of copper sulfide from brine in porphyry settings. However, the Henley et al experiments document anhydrous 1 atm gas reactions rather than more realistic hydrostatic simulations. To test if SO<sub>2</sub> reduction via anhydrite formation can efficiently trigger copper sulphide deposition, we experimentally reacted SO<sub>2</sub> gas

---

\* Research School of Earth Sciences, ANU

with calcite plus Cu-Fe-Na-Cl-brine at elevated pressure and temperature. An un-sealed gold capsule containing sodium sulphite was sealed inside an outer gold capsule containing calcite plus brine. Capsules were then placed in cold-seal vessels and run for two hour at 650° C and 1.5 kbar, and rapidly quenched. During the experiments sodium sulfite decomposes by the following reaction:  $\text{Na}_2\text{SO}_3 + 2 \text{H}^+ \rightarrow 2 \text{Na}^+ + \text{H}_2\text{O} + \text{SO}_2$ . Run products show chalcopryrite with anhydrite grown at the expense of calcite. Thus, for the first time, chalcopryrite has been experimentally synthesised by reaction between  $\text{SO}_2$  gas (the dominant sulfur component of magmatic gas) and brine. This highlights a key reaction in porphyry copper deposit formation and has obvious implications for the development of metal-bearing skarns.

## References

- Blundy, J, Mavrogenes, J, Tattich, B, Sparks, S. and Gilmer, A, 2015. Generation of porphyry copper deposits by gas-brine reaction in volcanic arcs. *Nature Geoscience*, v. 9, p.1–6.
- Henley, RW, King, PL, Wykes, JL, Renggli, CJ, Brink, FJ Clark, DA and Troitzch, T, 2015. Porphyry copper deposit formation by sub-volcanic sulphur dioxide flux and chemisorption, *Nature Geoscience*, v. 8, p. 210-215.
- Henley RW, Mavrogenes JA and Tanner D (2012) Sulfosalt melts and heavy metal (As-Sb-Bi-Sn-Pb-Tl) fractionation during volcanic gas expansion: the El Indio (Chile) paleo-fumarole. *Geofluids* DOI: 10.1111/j.1468-8123.2011.00357.x.

# The smoothness and shapes of chondrite-normalized Rare Earth Element patterns in basalts

by

Hugh St C O'Neill\*

The customary practice for displaying REE abundances is to normalize them to chondritic abundances, and then to plot these normalized abundances in order of atomic number,  $Z$ , although the 3+ ionic radius,  $r_{\text{REE}}$ , is proposed here as a preferable independent variable. In basalts, the resulting CI-normalized REE patterns usually appear smooth (excepting Eu), such that they may be fitted to polynomials in  $r_{\text{REE}}$  with three to five terms, depending on analytical precision. The polynomials can be re-arranged into an orthogonal form:

$$\ln \left( \frac{[\text{REE}]}{[\text{REE}]_{\text{CI}}} \right) = \lambda_0 + \lambda_1 f_1^{\text{orth}} + \lambda_2 f_2^{\text{orth}} + \dots$$

where  $f_1^{\text{orth}}$ ,  $f_2^{\text{orth}}$ , etc. are themselves polynomials of  $r_{\text{REE}}$ , chosen such that the coefficients  $\lambda_0$ ,  $\lambda_1$ ,  $\lambda_2$  etc. are not correlated with each other. The terms have a simple, intuitive meaning:  $\lambda_0$  is the average of the logarithms of the CI-normalised REE abundances; the term  $f_1^{\text{orth}}$  describes the linear slope of the pattern; that in  $f_2^{\text{orth}}$  describes the quadratic curvature, etc. For most basalts, fits using only three terms ( $\lambda_0$ ,  $\lambda_1$  and  $\lambda_2$ ) capture REE patterns to better than  $\pm 5\%$ . The  $\lambda_n$ , called the “shape coefficients”, can be used to compare the shapes of CI-normalized REE patterns quantitatively, allowing large numbers of data to be assessed, revealing trends not evident from studies of individual localities. Especially instructive are  $\lambda_2$  vs.  $\lambda_1$  diagrams. The usefulness of this approach is demonstrated using the REE patterns of common types of basalts from (mainly) oceanic settings: Ocean Floor Basalts (OFBs), Ocean Island Basalts (OIBs), and some Convergent Margin Basalts. It is shown that the global population of OFBs is characterized by a narrow dispersion of  $\lambda_0$  at a given MgO content, but with large variations of  $\lambda_1$  and  $\lambda_2$ . Convergent Margin Basalts have much greater variation of at a given [MgO], but most plot in the same area of the  $\lambda_2$  vs.  $\lambda_1$  diagram. OIBs are well separated from the OFB global array on this diagram, with Hawaiian shield basalts occupying a unique area.

Because REE mineral/melt partition coefficients are also smooth functions of  $r_{\text{REE}}$ , many mass-balance equations for petrogenetic processes that relate observed concentrations to initial concentrations,  $[\text{REE}]_0$ , such as batch or fractional melting, or crystallization, may be fitted to the same orthogonal polynomials:

$$\ln \left( \frac{[\text{REE}]}{[\text{REE}]_0} \right) = \psi_0 + \psi_1 f_1^{\text{orth}} + \psi_2 f_2^{\text{orth}} + \dots$$

The orthogonality ensures that all  $\lambda_n$  and  $\psi_n$  terms of the same order  $n$  sum independently of the terms of the other orders, such that  $\lambda_n = \lambda_n^\circ + \psi_n$ , where  $\lambda_n^\circ$  is the shape coefficient of the source or parent magma. On  $\lambda_2$  vs.  $\lambda_1$  diagrams, this approach can be used to relate the shapes of patterns in parental basalts to the shapes of the patterns of their sources, or differentiated basalts to their parental melts, by means of “petrogenetic process vectors” consisting of the  $\lambda_1$  and  $\lambda_2$  terms, which plot as vectors on the  $\lambda_2$  vs.  $\lambda_1$  diagrams. For example, the difference between OIBs and the global array of OFB can be shown to be due to garnet in the sources of OIBs.

The global array of OFBs require a remarkably constant degree of partial melting ( $F$ ) of a source with constant  $\lambda_0$  to produce their parental magmas, or a compensating correlation between  $F$  and source  $\lambda_n$ . Assuming a constant source, with previously suggested depleted mantle compositions,  $F$  is  $\sim 19\%$ , with the standard deviation of the population being only 2%. Hawaiian shield tholeiites are likely products of a couple percent melting at substantially higher pressures, perhaps straddling the garnet-to-spinel transition, of a source with REE patterns near the median of the REE patterns of OFB sources. Other OIBs come from even lower degrees of melting, usually of more light REE-enriched sources.

---

\* Research School of Earth Sciences, The Australian National University, Acton, ACT 2601, Australia

# Magnetotelluric imaging of the Earth across scales

by

Stephan Thiel\*

## Introduction

Exploration under cover remains one of the main impediments to mineral exploration in Australia. With a lack of conclusive mineral pointers from upper crustal and near-surface geophysical techniques, such as potential field methods, the push to understanding mineral systems across the entire lithospheric column provides a promising addition to mineral exploration packages. Additionally, the constraints on lithospheric architecture and insights into composition shed a crucial light on the tectonic setting mineral fertility corridors. With an increased understanding of a whole lithosphere approach to exploration (Griffin et al., 2013), deep probing geophysical techniques such as magnetotellurics (MT) (Thiel and Heinson, 2013; Heinson et al., 2006; Jones et al., 2009), seismic tomography (Rawlinson et al., 2014; Kennett and Salmon, 2012) as well as geochemical sampling of the sub-continental lithospheric mantle (SCLM) (Griffin et al., 2013; O'Reilly and Griffin, 2010) will play an increasingly important role in terrane-to-province selection of target areas for mineral exploration.

The illumination of crustal and sub-continental lithospheric mantle (SCLM) using geophysical techniques is largely restricted to seismic and magnetotelluric techniques. The flexibility of MT for craton-wide deployments to close-spaced high resolution surveys across mineral deposits highlights the technique's ability to image across all scales from depths of a few tens of metres to hundreds of kilometres. The sensitivity of MT to electrical resistivity stresses its importance in detection of usually minor conducting phases such as fluids and fluid precipitates (graphite, sulphide, mineralisation). Fluid pathways are often confined to structural boundaries characterised by changes in rheology, associated with gradients in density, magnetic susceptibility and elastic properties.

The AusLAMP SA program, funded in various stages by the Geological Survey of South Australia (GSSA), and University of Adelaide (UofA) has deployed over 200 long-period (5 s to 10 000 s) MT sites across the

state south of 28° latitude from the border with Western Australia to New South Wales and Victoria in the east. Currently, a joint project between GSSA, Geoscience Australia, and UofA is deploying another 54 MT sites across the Maralinga Tjarutja, Mamungari, and Far West Coast lands covering the Eucla and Officer Basin across the western margins of the Gawler Craton.

## AusLAMP SA long-period MT — illuminating the regional scale

In September 2014, the AusLAMP SA program commenced with the deployment of 50 km spaced long-period MT sites across the Woomera Prohibited Area (WPA) in the northern part of the Gawler Craton (Hand et al., 2007) and the south-east part of South Australia. The survey layout utilises pre-existing MT sites that are of high enough quality to be included into the AusLAMP database. A minimum requirement is that impedance responses are available for periods of up to 10 000 s ensuring penetration depths of the entire lithospheric column. The AusLAMP SA deployment uses the Auscope MT instruments housed at the University of Adelaide. Instruments record for more than 3 weeks and typically yield stable impedance responses from robust processing schemes (Chave and Thomson, 2004). The longer recording time compared to previous profile-type MT surveys significantly lowers noise levels, particularly for long periods.

The impedance data of the 156 AusLAMP MT stations across the Gawler Craton and margins, including 50 quality-selected long-period MT sites from previous surveys (Thiel and Heinson, 2013, 2010; Duan et al., 2010; Thiel et al., 2010; Heinson et al., 2006) are converted into the model domain using the smooth 3D non-linear conjugate gradient inverse code ModEM (Kelbert et al., 2014; Egbert and Kelbert, 2012). Preliminary models delineate the Archean core of the Gawler Craton represented by high resistivities (> 1000  $\Omega\text{m}$ ). Along its eastern margin extends a north-south oriented crustal low resistivity zone (few tens of  $\Omega\text{m}$ ) coincident with the eastern margin of the GRV and mineral prospects of the IOCG belt, including Olympic Dam. Contrary to previous conceptual models, the Olympic Dam IOCG belt is not connected to the IOCG prospects across the Yorke Peninsula from a lithospheric

---

\* Geological Survey of South Australia, Department of State Development, Adelaide, South Australia 5001

architecture point of view. Instead, the low crustal conductivity corridor extends in a south-westerly direction beneath the Gawler Range Volcanics and links to the north-south oriented crustal conductor across the Eyre Peninsula (White and Milligan, 1984).

Additionally, the conductive IOCG belt along the eastern margin of the Gawler Craton is connected to a mantle conductor situated beneath the Gawler Range Volcanics at depths between 100 km and ~200 km (Thiel and Heinson, 2013). Constant orientation of phase tensor ellipses for depths representative of the mantle conductor and higher directional misfit of the impedance data from 3D isotropic inversion suggests that the mantle conductor is anisotropic in nature. The low resistivity of 10  $\Omega\text{m}$  is too high to be caused by hydrogen in crystal lattice alone. Given the stability field of graphite and the depth extent of the conductor it may seem that it is a possible cause for the mantle conductor (Wang et al., 2013).

The geometry of the mantle and crustal conductivity pathways suggest that ~1590 Ma tectonic events played a significant role in the genesis of low resistivity. High-resolution 2D models across the Olympic Dam deposit show that low resistivity pathways are structurally controlled by Moho offsets and the brittle-ductile zone. It appears that the margin of the Gawler Craton exerts a primary architecture control on the emplacement of IOCG deposits in South Australia.

## References

- Alan D. Chave and David J. Thomson. Bounded influence magnetotelluric response function estimation. *Geophysical Journal International*, 157(3):988–1006, 2004.
- J. Duan, P.R. Milligan, and A. Nakamura. Magnetotelluric survey along the GOMA deepseismic reflection transect in the northern Gawler Craton to Musgrave Province, South Australia. In R. Korsch and N. Kositsin, editors, *GOMA (Gawler Craton-Officer Basin-Musgrave Province-Amadeus Basin) Seismic and MT Workshop 2010*, volume 2010/039, pages 7–15. Geoscience Australia, Record, 2010.
- Gary D. Egbert and Anna Kelbert. Computational recipes for electromagnetic inverse problems. *Geophysical Journal International*, 189(1):251–267, 2012.
- W. L. Griffin, G. C. Begg, and Suzanne Y. O'Reilly. Continental-root control on the genesis of magmatic ore deposits. *Nature Geoscience*, 6:905–910, October 2013.
- Martin Hand, Anthony Reid, and Liz Jagodzinski. Tectonic Framework and Evolution of the Gawler Craton, Southern Australia. *Economic Geology*, 102(8):1377–1395, 2007.
- G.S. Heinson, N.G. Direen, and R.M. Gill. Magnetotelluric evidence for a deep-crustal mineralizing system beneath the Olympic Dam iron oxide copper-gold deposit, southern Australia. *Geology*, 34: 573–576, 2006.
- Alan G. Jones, Rob L. Evans, Mark R. Muller, Mark P. Hamilton, Marion P. Miensopust, Xavier Garcia, Patrick Cole, Tiya Ngwisany, David Hutchins, C.J.S. Fourie, Hielke Jelsma, Shane Evans, Theo Aravanis, Wayne Pettit, Sue Webb, and Jan Wasborg. Area selection for diamonds using magnetotellurics: Examples from southern Africa. *Lithos*, 112:83–92, November 2009.
- Anna Kelbert, Naser Meqbel, Gary D. Egbert, and Kush Tandon. Modem: A modular system for inversion of electromagnetic geophysical data. *Computers & Geosciences*, 66(0):40 – 53, 2014.
- B. L. N. Kennett and M. Salmon. AuSREM: Australian Seismological Reference Model. *Australian Journal of Earth Sciences*, 59(8):1091–1103, 2012.
- Suzanne Y. O'Reilly and W.L. Griffin. The continental lithosphere-asthenosphere boundary: Can we sample it? *Lithos*, 120(1–2):1 – 13, 2010.
- N. Rawlinson, M. Salmon, and B.L.N. Kennett. Transportable seismic array tomography in southeast Australia: Illuminating the transition from Proterozoic to Phanerozoic lithosphere. *Lithos*, 189(0):65–76, 2014. ISSN 0024-4937. The lithosphere and beyond: a multidisciplinary spotlight.
- S. Thiel and G. Heinson. Crustal imaging of a mobile belt using magnetotellurics: An example of the Fowler Domain in South Australia. *Journal of Geophysical Research*, 115(B6):B06102, 2010.
- S. Thiel and G. Heinson. Electrical conductors in Archean mantle - result of plume interaction? *Geophysical Research Letters*, 40:2947–2952, 2013.
- S. Thiel, P. Milligan, G. Heinson, G. Boren, J. Duan, J. Ross, H. Adam, T. Dhu, T. Fomin, E. Craven, and S. Curnow. Magnetotelluric acquisition and processing, with examples from the Gawler Craton, Curnamona Province and Curnamona-Gawler Link transects in South Australia. In R. Korsch and N. Kositsin, editors, *South Australian Seismic and MT Workshop 2010*, pages 11–21. Geoscience Australia, Record, 2010/10, 2010.
- Duojun Wang, Shun-ichiro Karato, and Zhenting Jiang. An experimental study of the influence of graphite on the electrical conductivity of olivine aggregates. *Geophysical Research Letters*, 40(10): 2028–2032, 2013.
- White and P. Milligan. A crustal conductor on Eyre Peninsula, South Australia. *Nature*, 310: 219–222, 1984.

## Secular change in Archean crust formation recorded in Western Australia

by

Huaiyu Yuan\*

The formation mechanisms for early Archean continental crust are controversial. Continental crust may have accumulated via horizontal accretion in modern-style subduction zones or via vertical accretion above upper mantle upwelling zones. However, the characteristics of the continental crust changes at the transition between the Archean and Proterozoic eons, suggesting that continental crust did not form in subduction zones until at least the late Archean.

Here I use seismic receiver function data to systematically analyse the bulk properties (Yuan, 2015; Figure 1) of continental crust in Western Australia, which formed and stabilized over a billion years in the Archean. I find that the bulk seismic properties of the crust cluster spatially, with similar clusters confined within the boundaries of tectonic terranes. I discuss local Archean crustal growth models and show that the end-member models, the plume and subduction processes may have had a role in creating crust throughout the Archean. The thinner crust and lower Vp/Vs ratio in the Paleo-Archean Pilbara can be attributed to crustal formation above a plume that yields crustal melting and differentiation, and horizontal tectonics and accretion was the dominant process in the late Archean, and results in thicker crust and higher Vp/Vs ratios in the Yilgarn.

A correlation between crustal age and the bulk seismic properties of the crust reveals a trend (Figure 2): from about 3.5 Ga to the end of the Archean, the crust gradually thickened and simultaneously became more evolved in composition. I propose that this trend reflects the transition between crust dominantly formed above mantle plumes, to crust formed in subduction zones - a transition that may reflect secular cooling of Earth's mantle.

## References

- Cassidy, K. F. et al. A revised geological framework for the Yilgarn Craton, Western Australia. Geological Survey of Western Australia Record 2006/8, 8 (2006).
- Yuan, H. Secular change in Archean crust formation recorded in Western Australia. Nature Geosci 8, 808-813 (2015).

---

\* ARC Centre of Excellence for Core to Crust Fluid Systems, Department of Earth and Planetary Sciences, Macquarie University; Centre for Exploration Targeting, University of Western Australia; Geological Survey of Western Australia

Email: huaiyu.yuan@gmail.com

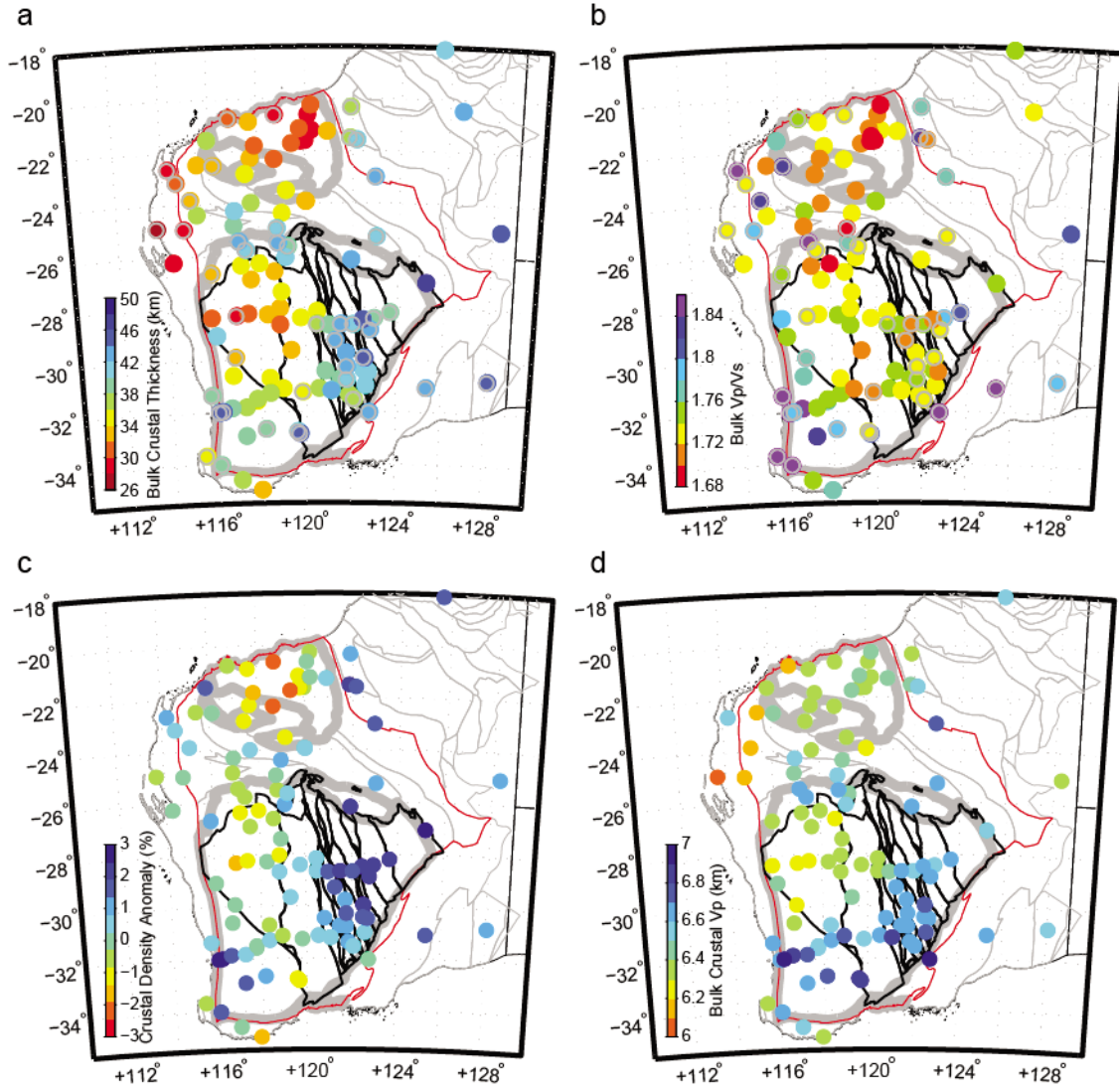


**Figure 1** Spatial distribution of the crustal observations in the Western Australian craton. a–d, Bulk crustal thickness (a),  $V_p/V_s$  ratio (b), crustal density anomaly<sup>2</sup> (c) and composite bulk crustal compressional wave (P-wave) velocity using the AuSREM crust model<sup>3</sup> (d). The measurements are color-coded and plotted at the seismic stations. The WA craton is contoured in red. The subdivisions of WA can be found in Fig. 2 and Supplementary Fig. 1 of Yuan (2015). The terrane boundaries in the Yilgarn craton are from Cassidy et al. (2015). In a and b, results from all available sites (good-quality sites, Supplementary Table 1 and Supplementary Fig. 5 (Yuan, 2015) and less-coherent sites marked with grey edge, Supplementary Table 2 and see Supplementary Section 2.1 in Yuan (2015) are plotted for completeness, but only the good-quality sites are used in interpretation.

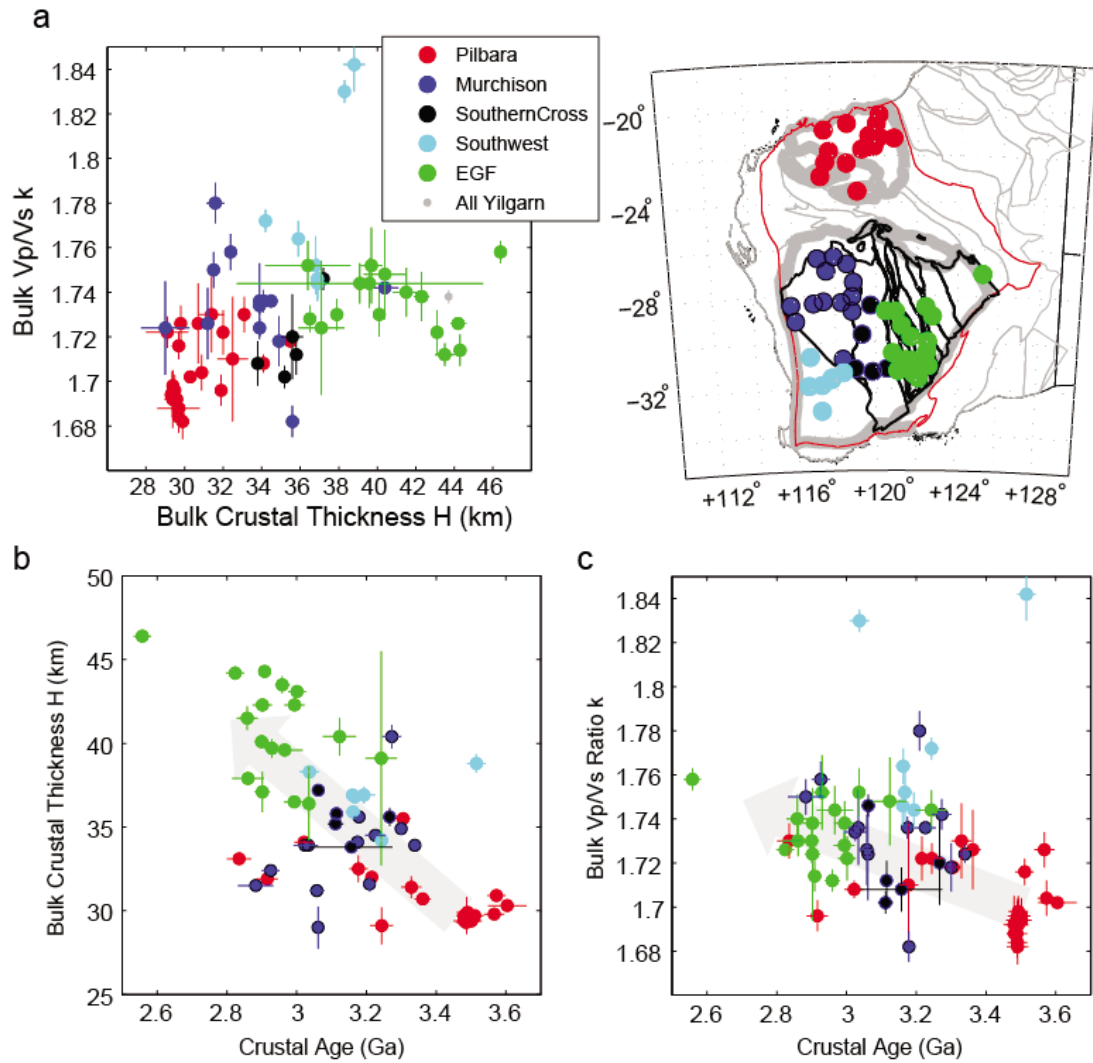


**Figure 2** Clustering and temporal variations in the WA crust. a–c, Clustering in the seismic measurements (a), the age correlation of the bulk  $V_p/V_s$  ratio (b), and the bulk crustal thickness (c). Stations for each subdivision are marked on the map (inset) and labelled in a. The measuring errors (see Methods and also Supplementary Section 2.2 in Yuan (2015)) of seismic observations and the errors associated with the isotopic ages<sup>48</sup> are indicated. Note the large deviation of the Southwest terrane and lack of robust measurements from the Narryer terrane, which are discussed in Supplementary Sections 3 and 4 in Yuan (2015).

# Trace element analysis on sulphides in olivine-phyric Shergottites: constraints on the behaviour of siderophile-chalcophile elements and sulphur in Martian magmatic systems

by

Raphael J. Baumgartner<sup>a</sup>, Marco L. Fiorentini<sup>a</sup>, David Baratoux<sup>b,c</sup>, Federica Zaccarini<sup>d</sup>, Jean-Pierre Lorand<sup>e</sup>, Ludovic Ferrière<sup>f</sup>, Kerim A. Sener<sup>g</sup>

Olivine-phyric Shergottites are Martian, mantle plume-related, mafic to ultramafic igneous rocks. Various proportions (up to 1 vol.%) of magmatic Fe-Ni (Cu) sulphide assemblages dominated by pyrrhotite are common constituents. They predominately occur embedded in plagioclase-free silicate glass or at multiple junctions between mesostasis silicates, and are interpreted to have segregated as discrete sulphide droplets upon cooling of their parental melts [1]. We report the first in-situ LA-ICP-MS trace element analyses on unaltered sulphides in a representative set of incompatible element-depleted olivine-phyric Shergottites (i.e., Y 980459, Tissint, DAG 476 and Dhofar 019), all of which presumably formed from a single, or very similar mantle/melt sources [2].

The analyses reveal siderophile-chalcophile element distributions and concentrations that can be reconciled with in-situ fractionation of discrete sulphides. The sulphides are devoid of platinum-group minerals (PGM), which can be explained by 1) the absence of PGM microcrystals in the parental melts, and 2) PGE contents too low to saturate and exsolve PGM. The sulphides in Y 980459, which presumably represents a primitive mantle melt [3], have significantly elevated Pd and lower Cu/Pd values, if compared with the more evolved DAG 476, Tissint and Dhofar 019. The observed differences can be explained by sulphide fractionation at varying stages during melt genesis, ascent and/or emplacement. Most probably, the variations reflect the segregation and loss

of sulphide upon emplacement of the primitive Y980459 specimen, and prior to crystallisation of DAG 476, Tissint and Dhofar 019.

## References

- [1] Lorand et al. (2005) *Met. Plan. Sci.* 40,1257-1273;
- [2] Treiman and Filiberto (2015) *Met. Plan. Sci.* 50,632-648; [3] Musselwhite et al. (2006) *Met. Plan. Sci.* 41,1271-129

---

a Centre for Exploration Targeting, ARC Centre of Excellence for Core to Crust Fluid Systems, The University of Western Australia, 6009 Crawley, Australia;

b Géosciences Environnement Toulouse, CNRS, IRD and University of Toulouse, 31400 Toulouse, France;

c Institut Fondamental d'Afrique Noire Cheikh Anta Diop, 5005 Dakar, Senegal;

d Department of Applied Geological Sciences and Geophysics, University of Leoben, 8700 Leoben, Austria;

e Laboratoire de Planétologie et Géodynamique de Nantes, Université de Nantes, 44322 Nantes, France;

f Natural History Museum Vienna, 1010 Vienna, Austria;

g Matrix Exploration Pty Ltd., 6112 Armadale, Australia

# Ruthenium in spinel from Chassignite and olivine-phyric Shergottite meteorites: constraints on the behavior of platinum-group elements and sulphur in Martian magmatic systems

by

Raphael J. Baumgartner<sup>a</sup>, Marco L. Fiorentini<sup>a</sup>, David Baratoux<sup>b,c</sup>, Ludovic Ferrière<sup>d</sup>, Marek Locmelis<sup>e</sup>, and Kerim A. Sener<sup>f</sup>

The Shergottite and Chassignite meteorites represent Martian, mantle-plume related, mafic to ultramafic igneous rocks ejected by asteroid/comet impacts. Magmatic spinel crystals (i.e., chromite and ulvöspinel) contained in the Chassignites NWA 2737 and Chassigny, as well as the olivine-phyric Shergottites Tissint and Dhofar 019, were analysed for the platinum-group elements (PGE) Os, Ir, Ru and Rh by in-situ LA-ICP-MS.

Aside from PGE-rich inclusions, chromites and ulvöspinel from both meteorite groups lack detectable concentrations of Os, Ir and Rh in solid solution (i.e., average detection limit of 7, 40, and 15 ppb, for Rh, Os, and Ir, respectively). Similarly, chromite and ulvöspinel from the olivine-phyric Shergottites is devoid of Ru (i.e. ~ 30-40 ppb detection limit). Detectable concentrations of Ru are restricted in chromites from the Chassignites (i.e., up to ~ 165 ppb, with the majority containing ~ 60-120 ppb Ru). These data demonstrate for the first time the partitioning of Ru in spinel from a planetary body other than the Earth.

Considering the contrasting affinity of Ru for sulphide ( $D_{\text{sulphide}} > 104$  [1]) relative to chromite ( $D_{\text{chromite}} = 30-120$  [2,3]), we link the Ru concentrations in the chromites from the Chassignites with their crystallisation from a silicate melt undersaturated in sulphide. We further note systematic changes in Ru concentrations, which can be reconciled with the continuous crystallisation of chromite (and accompanied sequestration of Ru) from a parental melt containing ~ 1-10 ppb Ru. The absence of detectable Ru concentrations in chromites and ulvöspinel

from the olivine-phyric Shergottites requires their crystallization from a melt relatively depleted in Ru with respect to the parental melt of the Chassignites, and/or 2) their crystallisation in contact with immiscible sulphides.

## References

- [1] Patten et al. (2013) *Chem. Geol.* 358,170-188;
- [2] Pagé et al. (2012) *Chem. Geol.* 41,1271-1290;
- [3] Brenan et al. (2012) *Chem. Geol.* 302-303,632-648

- 
- a Centre for Exploration Targeting, ARC Centre of Excellence for Core to Crust Fluid Systems, The University of Western Australia, 6009 Crawley, Australia;
  - b Géosciences Environnement Toulouse, CNRS, IRD and University of Toulouse, 31400 Toulouse, France;
  - c Institut Fondamental d'Afrique Noire Cheikh Anta Diop, 5005 Dakar, Senegal;
  - d Natural History Museum Vienna, 1010 Vienna, Austria;
  - e NASA Goddard Space Flight Center, 20771 Greenbelt, USA;
  - f Matrix Exploration Pty Ltd, 6112 Armadale, Australia;

## Cassiterite as a multiprocess recorder in Sn bearing systems

by

Jason Bennett<sup>1</sup>, Tony Kemp<sup>1</sup>, Steffen Hagemann<sup>1</sup>, Marco Fiorentini<sup>1</sup>

The 21st century is seeing an increased demand for rare metals such as Li, In, Nb, Ta, W and Mo. These elements are usually associated with Sn, which predominantly crystallises as cassiterite (SnO<sub>2</sub>). Cassiterite has the potential to open up a new research frontier for Sn-bearing polymetallic deposits with the development of modern high resolution in situ mass spectrometers. It is now possible to exploit the geochemical information in cassiterite as a process recorder of the physical, chemical and temporal mechanics of these mineralised systems. In order to highlight the potential of cassiterite as the new zircon of mineralised systems, a mineralogical, geochemical and isotopic study will be completed on cassiterite from a range of mineralised environments across multiple continents. This will be the first thorough study of its kind on cassiterite. The aim of this work is to establish the functionality of the cassiterite 'multi-tool' and its applications, precision, reliability and limitations.

This outcomes of this research will be achieved via; 1). A microgeochemical reconnaissance of cassiterite from multiple environments of formation, 2). Petrologic studies to determine the mineralogical and physiochemical controls on the trace element budgets outlined from above, 3). Thermodynamic and empirical modelling of trace element partitioning between coexisting phases during the evolution of the system, 4). Definition of the limitations of the U/Pb in cassiterite geochronometer, and 5). Identification and calibration for any potential geobarometer or geothermometers highlighted during the above research.

As of September 2015, 45 samples from 35 different localities have been gathered for this research project. The majority of these cover the main tin producing regions of Australia, with a few international samples (Bolivia, New Mexico, Cornwall). Additional samples will be sought further into the research. Some preliminary analyses from cathodoluminescence imaging of cassiterite shows zoning patterns, prominent (110) twin planes, and overprinting and breccia textures that are highly variable within the same deposit, as well as across localities.

Microprobe analyses of some of these are showing some distinct substitution trends, which appear to be mutually exclusive. Further early analysis by LA-ICP-MS also show a correlation between the Mn<sup>4+</sup> and Zr<sup>4+</sup> concentrations, indicating the existence of two thermobarometers in cassiterite. The uptake of 4+ cations should be theoretically controlled by the temperature and pressure of the system during crystallisation, similar to the Zr in rutile, Ti in zircon or Ti in quartz systems. Later analyses will also look at Sn<sup>4+</sup> in quartz, and these results will be compared with the Mn and Zr contents in cassiterite and calibrated against temperature-pressure data from fluid inclusions in co-existing quartz. This crude calibration can then be refined experimentally if the thermobarometers identified show significant promise in sensitivity and precision.

This new information will then be incorporated into existing models for Sn-bearing metallogenic systems, which will refine exploration search parameters allowing for improved targeting of new exploitable orebodies. In particular, the mutual exclusivity in minor element substitution trends may be exploitable for mineralisation style fingerprinting. Combined with temperature, pressure and time measurements, this may allow for highly efficient exploration targeting with detrital cassiterite in both alluvial and regolith settings.

---

<sup>1</sup> Centre for Exploration Targeting, The University of Western Australia

## Unravelling crustal growth and geodynamics in the Meso to Neoarchaeon using U-Pb-O isotopes in zircons and stratigraphic reconstructions from the Marmion Terrane (3.0 Ga)

by

**Björkman, K. E.<sup>1</sup>, McCuaig, T. C.<sup>1</sup>, Lu, Y. J.<sup>1</sup>, Kemp, A. I. S.<sup>1</sup>, Hollings, P.<sup>2</sup>**

A large proportion of today's continents are postulated to be underlain by Archaean continental lithospheric mantle. Therefore understanding the evolution of continental crust and mantle in the Archaean directly bears on our understanding of both earlier and subsequent development of the lithosphere. Older crust and lithosphere has been overprinted by subsequent tectono-thermal events making interpretations increasingly enigmatic with increasing age. We are using in-situ measurements of U-Pb-Hf-O isotopes in Meso- to Neoarchean igneous zircons to unlock the cryptic record of the growth of continental crust and mantle in the Marmion Terrane (3.02 – 2.68 Ga), Western Superior Craton, Canada, and explore relationships to mineral system distribution.

Uranium-Pb age determinations by SHRIMP show that the Marmion Terrane records near-continuous magmatism with coupled greenstone growth from 3.02 – 2.68 Ga. Age peaks occur at ~2.685, 2.73, 2.78, 2.83, 2.93, and 3.0 Ga. A tectonic mechanism such as incessant subduction or a long-lived oceanic plateau is invoked to account for the semi-continuous magmatism. These geodynamic scenarios have contrasting implications of continuous plate movement or a stagnant or slow-moving regime respectively.

The supracrustal record from 3.02 – 2.80 Ga is comprised of voluminous tholeiitic basalt, komatiitic basalt, and rare aluminum undepleted komatiite, all with an oceanic plateau geochemical affinity similar to the Ontong-Java plateau. Thin intercalated calc-alkaline felsic to intermediate volcanoclastic rocks occur throughout the sequence. At 2.8 Ga the Marmion Terrane was uplifted. Conglomerate channels eroded into the Trondjemite-Tonalite-Granodiorite (TTG) basement, and stromatolitic dolomite and iron formation was deposited. Pyroclastic aluminum depleted komatiite was deposited over the iron formation. Subsidence was followed by a change to more calc-alkaline basalt and andesite at the southern margin of the terrane at 2.74 – 2.72 Ga. Basin inversion accompanied

ongoing transpression during the Kenoran orogeny and late Timiskiming-type sedimentation was localised in synclinal axes of Mesoarchean greenstone belts and along the active southern margin of the terrane at 2.7 Ga.

These data support a shift in geodynamics at the Meso to Neoarchean transition. The dominantly tholeiitic mafic volcanism during the Mesoarchean indicates large degrees of partial melting of the mantle at depths above 8 GPa. The uplift evidenced by the supracrustal rocks at 2.8 Ga may reflect development of a buoyant lithospheric keel due to depletion by the preceding tholeiitic mafic volcanism, causing the succeeding melting event to occur at greater depths than 8 GPa. This was eventually followed by partial melting of a metasomatised mantle.

The last Archaean plutonic events in the terrane include post-tectonic <2.70 Ga area-extensive granodioritic and granitic crust-derived batholiths, and ~2.68 Ga late mantle derived intrusions (LMDI) with a Sanukitoid geochemical affinity. LMDI occur as ovate plutons throughout the Wabigoon Superterrane and the Quetico Basin. A heavy oxygen isotopic signature ( $\delta^{18}\text{O} \sim 7\text{‰}$ ) with respect to mantle signatures associated with zircons from sanukitoid rocks preserve convincing evidence for a supracrustal component. It remains unclear if supracrustal rocks were part of the source or were assimilated upon ascent.

This study is showing that mapping isotopic boundaries has potential to illustrate prospective lithospheric architecture for TTG-hosted gold mineralisation and Ni-Cu-PGE hosted by LMDI. Nickel-Cu-PGE mineralisation is localised in gabbroic to monzodiorite phases of LMDI along external margins of the Marmion Terrane as revised by this study. Areas of TTG complexes that have focused later thermal events also host the significant gold mineralisation. Gold occurs in the oldest phases of the TTG near the steepest age gradients, including the 10.7 Moz Hammond Reef deposit.

1 Centre for Exploration Targeting and ARC Centre of Excellence for Core to Crust Fluid Systems (CCFS), School of Earth and Environment, The University of Western Australia, M006, 35 Stirling Highway, Crawley, WA 6009, Australia.

2 Centre for Sustainable Mining and Exploration, Department of Geology, Lakehead University, Thunder Bay, Ontario, P7B 5E1

# The Arabian-Nubian Shield (8.50-5.50 Ga) as an analogue for the Birimian Orogen (2.35-2.05 Ga)?

by

Mikael Grenholm\*

Many comparative studies have been conducted between past and present orogenic belts in order to gain insights into geodynamics, metallogeny, and secular change through Earth's history. This study concerns the Neoproterozoic (0.85-0.55 Ga) Arabian-Nubian Shield in NE Africa and the western Arabian Peninsula, and the Paleoproterozoic (2.35-2.05 Ga) Birimian Orogen in West Africa, and it is argued here that these two orogens are analogous. This applies to both the geodynamic processes associated with their formation, and the global context in which the orogens developed.

Both the Arabian-Nubian Shield and the Birimian Orogen are largely juvenile accretionary-collisional orogens, which experienced an equivalent evolution. This included an initial accretionary phase (ca. 200 Myr) with extrusive and intrusive volcanic arc magmatism, and HP-LT metamorphism (12-14 Kbar, 500-550 C°). This was followed by a collisional phase (ca. 150-100 Myr), associated with a shift towards more evolved magmatism and crustal thickening, with contemporaneous exhumation of middle crust and the establishment of large sedimentary and volcano-sedimentary basins.

From a wider perspective, both the Arabian-Nubian Shield and the Birimian Orogen have the same relationship to two unique sets of positive excursions in  $\delta^{13}\text{C}$  and  $^{87}\text{Sr}/^{86}\text{Sr}$ , as measured in marine carbonates. These excursions occurred during the Neoproterozoic-Paleozoic and Paleoproterozoic Eras, respectively, and have the same magnitude, duration and relative timing. The C and Sr isotopic composition of marine carbonates reflect the composition of the global oceans, which is inferred to be strongly controlled by tectonic processes, involving uplift, weathering, volcanism and sedimentation. As such, the C and Sr isotopes can be seen as a record of global tectonics through time.

The Arabian-Nubian Shield and the coeval C and Sr excursions formed within the context of the ca. 1.0-0.3 Ga cycle between the supercontinents Rodinia and Pangea. Because of its similarities with the Arabian-Nubian Shield, it can be inferred that the Birimian Orogen formed in an analogous global context, involving the break-up of a supercontinent equivalent to Rodinia at ca. 2.5 Ga, and the assembly of a supercontinent equivalent to Pangea at ca. 1.8 Ga.

The similarities between the Arabian-Nubian Shield and the Birimian Orogen mean that the former may act as an analogue for the latter. As such, the Arabian-Nubian Shield may provide insights into geodynamic processes and the paleogeographic setting during the assembly of the Birimian Orogen. Furthermore, the similarities between the two orogens opens up the possibility that they may contain equivalent styles of mineralization, and that knowledge of the lithological associations and structural setting of a particular deposit in one orogen can be used to explore for that style of deposit in the other orogen.

---

\* Centre for Exploration Targeting (M006), University of Western Australia, 35 Stirling Highway, Crawley, Perth, Western Australia 6009, Australia.

## In-situ U-Pb, O and Hf isotopic compositions of detrital zircons from the North Australian Craton

by

Linda Iaccheri\*

The process of continents assembling and crustal growth is controversial, because the mechanism of continental crust formation and evolution remains poorly understood.

The global compilation of juvenile zircon ages and their relative abundance shows distinct peaks. These peaks are inferred to represent episodic crustal growth throughout the Earth's history. However, there is a long withstanding argument that the peak distribution might be an artifact of preferential preservation.

The detrital zircon age spectra from Paleoproterozoic sediments from the North Australian Craton is interpreted to reflect the erosion of a section of continental crust that formed during two major thermal events: at ~2.5 Ga and ~1.87 Ga, which correlate with two significant peaks of the global zircon record.

The coupled oxygen and Hf isotope compositions for the detrital zircons of both events shows predominance of reworking of older crust, with limited continental crust growth at 2.5 Ga and no evidence for crustal growth at 1.87 Ga.

While the provenance of detrital zircons of both age populations can be traced back to local sources, Hf and O-isotopes clearly show two different and independent processes of crustal formation and evolution.

The results of this study show that the 1.87 Ga zircon population, and hence crust, was not generated by reworking of the ~2.5 Ga old crust, represented by the older zircon record. Moreover, the absence of correlation between Hf and O-isotope signatures implies no connection between crustal age of the source, low temperature alteration and magmatic processes. These findings question the current geodynamic understanding of the region and processes of crustal evolution in general. Overall, this implies that ancient crustal growth is not simply driven by reworking of older crust and different degrees of juvenile melt contributions.

---

\* In collaboration with Geoscience Australia and GSWA

# Geochronology and lithostratigraphy of the Siguiri district: implications for gold mineralisation in the Siguiri Basin (Guinea, West Africa)

by

Erwann Lebrun<sup>1</sup>, Nicolas Thébaud<sup>2</sup>, John Miller<sup>1</sup>, Julien Bourget<sup>2</sup>,  
Stanislav Ulrich<sup>3</sup>, and Ockert Terblanche<sup>3</sup>

The Siguiri Basin is located in the north-western part of the Paleoproterozoic Baoulé-Mossi domain of the South West African Craton. The Baoulé-Mossi domain was accreted against the Archean Kénéma-Man domain (in the south-west of the SWAC) during the Eburnean orogeny between ca. 2200 and 2040 Ma (Abouchami et al. 1990; Egal et al. 2002; Thiéblemont et al. 2004; Davis et al. in review 2015). The Siguiri Basin is one of the biggest metasedimentary basins of the SWAC (~ 40,000 km<sup>2</sup>) and hosts the world-class orogenic gold district of Siguiri (Lebrun et al. in press 2015a).

The lithostratigraphy of the Siguiri Basin was mapped by the French geological survey (BRGM) as a dominantly homogeneous package of undifferentiated sediments (Egal et al. 1999). These sediments were interpreted to have deposited during the Lower Birimian and then intruded by late Eburnean igneous rocks at ca. 2075 Ma (Egal et al. 1999; Egal et al. 2002; Feybesse and Milési 1994; Feybesse et al. 1999; Milési et al. 1989).

New ages and lithostratigraphic observations from the Siguiri district result in a revision of the Siguiri Basin stratigraphy. Three distinct metasedimentary formations are recognized in the district. The Balato and Fatoya formation form a basal regressive sequence, overlain by the Kintinian formation. This last formation is dominated by shale with a stack of polymict conglomeratic interbeds at its base. These conglomerates can be mapped throughout the entire Siguiri Basin and are interpreted to represent allolostromes. The maximum age of sedimentation of these three formations were dated at 2113±10, 2113±5 and 2120±5 Ma respectively. The minimum age of deposition of all these sediments is constrained by cross-cutting volcanic rocks dated at

2092±5 Ma. Put into the South West African Craton context, the sedimentary facies and geochronology of the Kintinian sediments suggest these are “late basin” sediments deposited during the early phases of the Eburnean orogeny, and highlight the fundamental structures controlling the early architecture of the Siguiri Basin and the location of major gold deposits. This study (Lebrun et al. in press 2015b) gives new insights into the tectonic evolution of the Basin and highlights the controls on the world-class orogenic gold Siguiri district location.

## Acknowledgements

This project is funded by AngloGold Ashanti Limited. Eddie Connell, Shawn Kitt, Katharina Wulff and Craig Duvel are acknowledged for providing site access, support and inspiring discussions. The authors also acknowledge the facilities, and the scientific and technical assistance of the Australian Microscopy & Microanalysis Research Facility at the Centre for Microscopy, Characterisation & Analysis, the John de Laeter Centre for Isotope Research, The University of Western Australia and Curtin University.

## References

- Abouchami W, Boher M, Michard A and Albaredé F (1990) A Major 2.1 Ga Event of Mafic Magmatism in West Africa - an Early Stage of Crustal Accretion. *J Geoph Res-Solid Earth and Planets* 95:17605-17629
- Davis J, Miller J, Thébaud N, McCuaig C, Begg G, Jessel, M, Hein K, Baratoux L and Perrouy S (in review 2015) Craton-scale lithostratigraphic correlation as an insight for the geodynamic evolution of the South West African Craton. *Precamb Res*
- Egal E, Lahondère D, Costea A C, Diabate B, Diallo A, Diallo A B, Diallo S, Gaye F, Iliescu D and Minthe D (1999) Carte géologique de la Guinée à 1/200 000 ; Feuille Siguiri. BRGM
- Egal E, Thiéblemont D, Lahondère D, Guerrot C, Costea C A, Iliescu D, Delor C, Goujou J, Lafon J, Tegye M, Diaby S and Kolie P (2002) Late Eburnean granitization and tectonics along the western and northwestern margin of the Archean Kénéma–Man domain (Guinea, West African Craton). *Precamb Res* 117:57-84
- Feybesse J, Bangoura A, Billa M, Costea A, Diabaté B, Diaby S, Diallo A, Diallo S, Diallo A and Egal E (1999) Notice explicative de la Carte géologique de la Guinée à 1/200 000, Feuille no. 19, Kankan. BRGM, DNRGH, Ministère des Mines, de la Géologie et de l'Environnement, Conakry, Guinée, 27 p

1 Centre for Exploration Targeting and ARC Centre of Excellence for Core to Crust Fluid Systems, School of Earth and Environment, Robert Street Building, M006, The University of Western Australia, 35 Stirling Highway, Crawley, WA, 6009, Australia

2 Centre for Petroleum Geoscience and CO2 Sequestration, School of Earth and Environment, M004, The University of Western Australia, 35 Stirling Highway, Crawley, WA, 6009, Australia

3 AngloGold Ashanti Ltd - Brownfields Exploration Technical Hub - Continental Africa Region, 44 St George Terrace, Perth, WA, 6000, Australia

- Feybesse J-L and Milési, J-P (1994) The Archean/Proterozoic contact zone in West Africa: a mountain belt of décollement thrusting and folding on a continental margin related to 2.1 Ga convergence of Archean cratons?. *Precamb Res* 69:199-227
- Lebrun E, Thébaud N, Miller J, Ulrich S, Bourget J and Terblanche O (in press 2015b) Geochronology and lithostratigraphy of the Siguiri district: implications for gold mineralisation in the Siguiri Basin (Guinea, West Africa). *Precamb Res*
- Lebrun E, Ulrich S, Miller J, Thébaud N and McCuaig C (in press 2015a) The world-class Siguiri gold district, Siguiri Basin, Guinea (West Africa): Stress switches within an orogenic gold system. *Econ Geol*
- Milési J P, Feybesse J L, Ledru P, Dommanget A, Ouedraogo M F, Marcoux E, Prost A, Vinchon C, Sylvain J P, Johan V, Teguey M, Calvez J Y and Lagny P (1989) Les minéralisations aurifères de l'Afrique de l'Ouest. Leurs relations avec l'évolution lithostructurale au Protérozoïque inférieur. *Chron rech min* 497:3-98
- Thiéblemont D, Goujou J C, Egal E, Cocherie A, Delor C, Lafon J M and Fanning C M (2004) Archean evolution of the Leo Rise and its Eburnean reworking. *J Afric Earth Sci* 39:97-104

# The tectono-magmatic evolution of the Kédougou-Kénieba inlier, West Africa: new insights from the Sadiola-Yatela gold district

by

Quentin Masurel<sup>1\*</sup>, Nicolas Thébaud<sup>1</sup>, John Miller<sup>1</sup>, Stanislav Ulrich<sup>2</sup>

Paleoproterozoic supracrustal and intrusive rocks in the West African Craton provide a complete record of crustal growth. The Kédougou-Kénieba inlier is the westernmost exposure of Birimian (ca. 2250-2050 Ma) crust in the West African Craton and a world-class gold province. The northeastern part of the Kédougou-Kénieba inlier hosts the ~15 Moz Sadiola-Yatela gold district. The geological setting of this part of the inlier, however, remains poorly-constrained to date. The study of igneous rocks in that region appears critical not only to unravel the tectono-thermal evolution of the Kédougou-Kénieba inlier, but also in terms of mineral system whereby gold deposits are viewed as local expressions of orogen- to lithospheric-scale processes. This study presents the structural framework, whole rock geochemistry and geochronology of representative magmatic rocks from the Sadiola-Yatela region. The data indicate that these rocks have undergone polycyclic deformation, which included a period of thrusting tectonics responsible for crustal thickening ( $D_1$ - $D_2$ ), followed by a period of transcurrent tectonics accommodating oblique convergence ( $D_3$ - $D_4$ ). The  $D_2$  and  $D_3$  events represent the principal imprint of the Eburnean orogeny in the region and were responsible for massive magmatic addition. The Eburnean intrusive rocks display a temporal evolution from syn- $D_2$  (ca. 2115-2080 Ma) calc-alkaline metaluminous plutons (e.g., diorite, hornblende-granodiorite) to syn- $D_3$  (ca. 2080-2060 Ma) peraluminous high-K granites (e.g., biotite-monzogranite). The bulk of orogenic gold mineralisation in the region occurred during  $D_3$ , with hydrothermal fluid circulation along the sinistral regional-scale shear zones and steep NNE-trending shears connected to structural traps in the adjacent basins and volcano-plutonic belts. These results suggest that the late Eburnean tectono-thermal event likely provided the geodynamic engine that empowered orogenic gold mineralisation in the Kédougou-Kénieba inlier.

---

1 Centre for Exploration Targeting, The University of Western Australia, 35 Stirling Highway, Crawley, WA.

2 AngloGold Ashanti Australia Limited, Asset Development - Brownfields, 44 St. Georges Terrace, Perth, WA.

\* Corresponding author: qmasurel@hotmail.com

# Melt generation during failed rift development – Insights from numerical modeling

by

**Mark A. Munro<sup>1</sup>, Weronika Gorczyk<sup>1</sup>, Chris Wijns<sup>2</sup>, Bruce Hobbs<sup>1,3</sup>, Alison Ord<sup>1</sup>**

Rifting is a fundamental geodynamic process associated with thinning of the Earth's lithosphere. These zones give rise to high heat flow, enhanced geothermal gradients and decompression melting, promoting melt generation. In its extreme form, protracted periods of rifting lead to continental (and super-continental) breakup via the development of oceanic basins, passive margins, oceanic crust production and seafloor spreading. Alternatively, bulk extension may cease in advance of seafloor spreading, resulting in a 'failed rift'.

In many geodynamic settings, phases of extension and rifting follow prior episodes of continental collision and amalgamation. Post-collisional intra-cratonic suture zones represent zones of intense shearing and strong mantle lithosphere metasomatism (Gorczyk et al., 2013). Consequently, these suture zones possess significantly different rheological and chemical properties (Ranalli, 1995) to the more competent terranes they are sandwiched between. These pre-existing weaknesses therefore respond differently during subsequent bulk extension, serving as a locus for strain.

Numerical modeling (Gerya & Yuen, 2007) of the behaviour of different post-collisional suture architectures under imposed bulk extension shows that significant volumes of mafic melt may be emplaced into the upper and lower crust even in scenarios where rifts ultimately fail. In the upper crust, this is linked with in-situ upper crustal melting. Under the right conditions, this may also be associated with the generation of lower crustal derived melts along the Moho at the interface with zones of pre-existing sheared lithospheric mantle. Lower crustal melts are also produced at the base of emplaced mafic plutons. More spatially extensive areas of prior mantle lithosphere metasomatism and shearing lead to more rapid rates of lithospheric thinning.

## References

- Gerya, T.V., Yuen, D.A. Robust characteristics method for modelling multiphase visco-elasto-plastic thermo-mechanical problems. *Physics of the Earth and Planetary Interiors* 163, 83–105 (2007).
- Gorczyk, W., Hobbs, B., Gessner, K., Gerya, T. Intracratonic geodynamics. *Gondwana Research* 24, 838–848 (2013).
- Ranalli, G. *Rheology of the Earth*. Chapman and Hall, London, 413pp (1995).

---

<sup>1</sup> Centre for Exploration Targeting, the University of Western Australia, Crawley, Western Australia, Australia

<sup>2</sup> First Quantum Minerals Ltd, West Perth, Western Australia, Australia

<sup>3</sup> CSIRO Earth and Resource Engineering, Bentley, Western Australia, Australia

# **Crustal Architecture and Under Cover Exploration: The Granites – Tanami Orogen Example**

by

**David B Stevenson<sup>1\*</sup>, Linda M Iaccheri<sup>1</sup>, T Campbell McCuaig<sup>1</sup>, Leon Bagas<sup>1</sup>, and Alan R A Aitken<sup>2</sup>**

Understanding the nature of the lithosphere and its crustal architecture is vital in the successful execution of regional mineral exploration under cover. Mapping of crustal architecture is achieved by integrating regional scale geophysical datasets with geological knowledge. In this study, we use the Paleoproterozoic Granites – Tanami Orogen (GTO) of central Australia as a natural laboratory to test the relationship between mineral systems and crustal architecture, and illustrate how these associations aid vectoring in on undiscovered resources under cover.

The GTO is a significant gold producing province. Gold mineralisation is hosted within the mid-Paleoproterozoic stratigraphy of the Tanami Group and is associated with late Paleoproterozoic deformation. Deep weathering profiles and cover sequences from Neoproterozoic to Paleozoic obscure much of the Tanami Group within the GTO. Consequently, the majority of gold discoveries

within the orogen occur in or near surface exposures of the Tanami Group. The interpretation of crustal scale 2D reflection seismic data identifies inverted basin architecture within the orogen, although the sparsity of seismic sections does not allow for the 3D mapping of this basin architecture at a regional scale. In this study we couple gravity, magnetic and seismic interpretation with geophysically constrained forward modelling to map out the GTO's crustal architecture and place its mineral systems within this architectural framework. We display how this integrated geology and geophysical approach to map crustal architecture is a cost effective technique to improve success in under cover mineral exploration.

---

1 Centre for Exploration Targeting and ARC Centre for Excellence for Core to Crust Fluid Systems (CCFS), The School of Earth and Environment, The University of Western Australia, 35 Stirling Highway, Crawley, WA 6009, Australia

2 Centre for Exploration Targeting, The School of Earth and Environment, The University of Western Australia, 35 Stirling Highway, Crawley, WA 6009, Australia

## Kimberlitic Plumbing System: One-Time Incident or Long-Term Relation?

by

**Irina Tretiakova<sup>1</sup>, Elena Belousova<sup>1</sup>, Vladimir Malkovets<sup>1,2,3</sup>, William Griffin<sup>1</sup>,  
Sandra Piazzolo<sup>1</sup>, and Norman Pearson<sup>1</sup>**

Kimberlitic pipes are not only economically important source of diamonds, but also represent natural drill holes providing samples from the whole sequence of levels from the mantle to the surface. Kimberlite eruption is known to be an extremely rapid event that can deliver xenoliths and xenocrysts relatively unaltered.

The Nurbinskaya pipe, in the Nakyn kimberlite field in the eastern Siberian Craton is one of the most diamond-rich kimberlites of the Siberian Craton. The pipe is located within the Vilui-Markha deep fault zone, a NE-trending structure associated with the middle Paleozoic Vilui rift system. All four kimberlite pipes (Maiskaya, Markhinskaya, Botuobinskaya and Nurbinskaya) in this field are diamondiferous. The kimberlites intruded into early Paleozoic terrigenous-carbonate sequences and are covered by 30-80 m of Jurassic terrigenous sediments.

An age of 364 Ma for the Nurbinskaya and Botuobinskaya kimberlites has been determined previously by Rb-Sr dating of kimberlitic phlogopite. This age falls into the 353-367 Ma range defined as the main emplacement event of Siberian diamondiferous kimberlites.

More than 150 zircon grains were collected from a heavy mineral concentrate of crushed whole-rock kimberlite from the Nurbinskaya pipe. All grains are clear, transparent, yellowish or brownish in color and 2-5 mm in size. The grain shapes are sub-rounded without crystal faces, which is typical of kimberlitic zircons.

Five grains have an unusual "mosaic" internal structure revealed by CL imaging. These were selected for more detailed investigation using EBSD analysis, U-Pb SHRIMP dating and analyzing of O-isotopes and trace element composition. Several grains without such structural features have been used for comparison.

The U-Pb dating defined two main age populations: Devonian and Archean. The younger population of zircons (26 analyses) shows ages ranging between 365 Ma and 375 Ma and yields a weighted average age of  $370.7 \pm 2.3$  Ma (MSWD = 0.28, probability = 0.998). The older population (156 analyses) ranges from 2681 to 2727 Ma with a weighted average age of  $2708.5 \pm 8.9$  Ma (MSWD = 0.59, probability = 0.91).

In contrast to the undeformed grains, which show identical (within analytical precision) ages within a single grain, each of three zircon grains with mosaic structure revealed a significant variation in age in different analytical spots within the grain. Thus, two analyses of grain NU-19-03 showed a remarkable age difference:  $404 \pm 10$  and  $518 \pm 12$  Ma. The range in age within grains NU-25-08 and NU-26-08 was less significant (383 and 414 Ma and 370 and 392 Ma correspondingly), but still outside the analytical error.

All analyzed grains reveal chondrite-normalized patterns of trace element abundances typical for zircons, with depletion in light rare earth elements and enrichment in heavy rare earth. However, the concentrations of trace elements are relatively low and rarely reach thousand-ppm levels. The REE patterns are similar in shape for both populations, but zircons from Devonian population are more depleted than Archean ones, especially in HREE. A characteristic feature of these grains is the almost total absence of Eu-anomaly. The difference in trace-element composition of blocks and interblock material of mosaic grains is visible, but not significant. Thus, REE patterns of blocks are closer to those of Archean zircons, while interblocks have more depleted composition. The variations in concentrations of some elements are just slightly outside of the analytical error, so the trace-element compositions of both blocks and interblocks could be considered as very similar. According to CART statistical classification all analyzed grains have trace-element composition similar to zircons coming from mantle-derived rocks (carbonatite or kimberlite).

Hf-isotope systematics were analyzed in 30 grains. Undeformed grains reveal a significant difference in isotopic composition between two main age populations. Young zircons have positive  $\epsilon_{\text{Hf}}$  typical for zircons from rocks with significant juvenile component, while  $\epsilon_{\text{Hf}}$  values of the ancient grains are close to 0 (-4 to +2.7).

- 
- 1 ARC Centre of Excellence for Core to Crust Fluid Systems (CCFS) and GEMOC, Dept. of Earth and Planetary Sciences, Macquarie University, Sydney, Australia
  - 2 V.S. Sobolev Institute of Geology and Mineralogy SB RAS, Novosibirsk, Russia
  - 3 The Pheasant Memorial Laboratory for Geochemistry & Cosmochemistry, Institute for Study of the Earth's Interior, Okayama University, Misasa, Tottori, Japan

Mosaic grains in contrast reveal extremely negative  $\epsilon_{\text{Hf}}$  values (up to -34.4). The calculated model ages of mosaic zircons and grains from Archean population are within the range 3.1-3.3 Ga. Moreover, both groups fit perfectly on the crustal evolution line with initial  $\text{Lu}/\text{Hf}=0.015$ .

Thus, two main age population were found among mantle-derived zircons from the Nurbinskaya pipe - Archean and Devonian. Zircon grains with "mosaic" internal structure are the link between these two major stages. U-Pb dating and isotopic systematics indicate that "mosaic" zircons originally crystallized in the Archean, but were recrystallized at 410-450 Ma. They were brittlely deformed and instantaneously healed at the time of kimberlite eruption (360-370 Ma). Thus, this research shows that kimberlitic pipes commonly suggested as a result of a single-time magmatic event could have much more complicated history starting long time before the eruption. Zircons allow us to clearly track several episodes of melting the similar part of the mantle produced magmas with close composition which then were driven into the crust and finally to the surface by the same "plumbing system".

# Can auriferous fluids produce their own pathways via porosity forming reactions? An insight from the Mick Adam gold deposit, Yilgarn Craton, Western Australia

by

James Warren<sup>1</sup>, Adam Bath<sup>2</sup>, Nicolas Thébaud<sup>3</sup>, Chris Kirkland<sup>4</sup>, John Walshe<sup>5</sup>

The Mick Adam gold deposit, the largest deposit within the 2.4 Moz Castle Hill gold camp, is located in the Coolgardie Domain of the Archean Yilgarn Craton. The Castle Hill gold camp is spatially associated with a regional pluton called the Kintore Tonalite. A number of techniques were used to define the alteration and chemical evolution of the Mick Adam deposit and, integrated with the structural history of the deposit, we were able to establish a paragenetic sequence of events. Analytical methods used during this study include drill-core logging, whole-rock geochemistry, TESCAN Integrated Mineral Analyser (TIMA) scanning electron microscopy (SEM), High-resolution X-Ray Computed Tomography (HRXCT), titanite geochronology and thermometry, and carbon and sulphur isotopic analysis. The age of magmatic titanite indicate the Kintore Tonalite was emplaced at c. 2708 ± 35 Ma, which is within error of published zircon U-Pb age data. The Kintore Tonalite was subsequently intruded by feldspar phyric, porphyry intrusive units which caused wide spread episyenitisation of the Kintore Tonalite, with a major observation being the generation of significant porosity, between approximately 8-12% of the rock volume. Episyenitisation occurred via the method of interface-coupled dissolution-precipitation. Episyenite zones are characterised by the pseudomorphic albitisation of previously andesine rich plagioclase, and a strong association with rutile. Temperatures, from titanite thermometry and isotope data, indicate that the episyenitisation event occurred at temperatures between

500-600°C, as a result of the circulation of alkaline, high-CO<sub>2</sub> fluids. Episyenitisation was followed by vein development and mineralisation. Gold bearing quartz-biotite-calcite veins have a strong alteration selvage, with complete albitisation of previously andesine rich plagioclase. Pyrite, with pyrrhotite intergrowths, rutile and titanite form the ore bearing assemblage within, and on the margin of, the mineralised veins. Gold is observed to have three habits in the Mick Adam deposit, including (1) quartz vein hosted, coarse grain gold (0.3-1mm), observed either as free gold, or gold associated with telluride group minerals, (2) free gold located in albite altered vein selvages, or in albite altered fault zones, with no observed relationship to telluride group minerals, and (3) fine grain gold (< 100µm), associated with tellurobismuthite and rutile, located in the strained, chloritised centre of biotite stylolites. Hydrothermal titanite, from mineralised samples, returns an age of 2579 ± 55 Ma. Fluid P, T, X conditions of mineralisation are interpreted to have been similar to those interpreted for the earlier episyenitisation event. We propose a model where by the early episyenitisation event creates a permeability network for the subsequent flow of hydrothermal fluids during mineralisation. We propose a possible magmatic fluid source for the episyenitisation and mineralisation events.

---

1 Centre for Exploration Targeting, Robert Street Building, M006, The University of Western Australia, 35 Stirling Hwy, Crawley, WA, 6009, Australia.

Phoenix Gold Ltd., 73 Dugan St, Kalgoorlie, Western Australia 6430

2 CSIRO Mineral Resources Flagship, PO Box 1130 Bentley, Western Australia 6102, Australia

3 Centre for Exploration Targeting, Robert Street Building, M006, The University of Western Australia, 35 Stirling Hwy, Crawley, WA, 6009, Australia.

4 Centre for Exploration Targeting, Curtin University of Technology, Bentley Campus, WA, 6102, Australia

5 CSIRO Mineral Resources Flagship, PO Box 1130 Bentley, Western Australia 6102, Australia

This Record is published in digital format (PDF) and is available as a free download from the DMP website at  
<[www.dmp.wa.gov.au/GSWApublications](http://www.dmp.wa.gov.au/GSWApublications)>.

Further details of geological products produced by the Geological Survey of Western Australia can be obtained by contacting:

Information Centre  
Department of Mines and Petroleum  
100 Plain Street  
EAST PERTH WESTERN AUSTRALIA 6004  
Phone: +61 8 9222 3459 Fax: +61 8 9222 3444  
[www.dmp.wa.gov.au/GSWApublications](http://www.dmp.wa.gov.au/GSWApublications)

2<sup>ND</sup> LITHOSPHERE WORKSHOP  
19–20 NOVEMBER 2015  
THE UNIVERSITY OF WESTERN AUSTRALIA

